Marine Pollution Bulletin 186 (2023) 114478

Contents lists available at ScienceDirect

Marine Pollution Bulletin

journal homepage: www.elsevier.com/locate/marpolbul

Increased barium levels in recent marine sediments from the Norwegian and Barents Seas suggest impact of hydrocarbon drilling and production

Hallvard Haanes [a,*], Henning K.B. Jensen [b], Aivo Lepland [b], Hilde Elise Heldal [c]

[a] Norwegian Radiation and Nuclear Safety Authority, P.O. Box 55, Østerås, Norway
[b] Geological Survey of Norway, P.O. Box 6315, Torgarden, NO-7491 Trondheim, Norway
[c] Institute of Marine Research, P.O. Box 1870, Nordnes, NO-5817 Bergen, Norway

ARTICLE INFO

Keywords:
Barium
Hydrocarbon drilling and production
Discharge
Impact
Marine sediments

ABSTRACT

Barium (Ba) in recent marine sediments can originate from natural and anthropogenic sources including discharges from the oil and gas industry. In this study, we use data from the Norwegian and Barents Seas to assess whether Ba in recent marine sediments has increased due to these discharges. To account for Ba in detrital material, we normalise all samples with respect to aluminosilicate by calculating an enrichment factor. We use statistical modelling to control for parameters related to sedimentation. We present results that suggest increased Ba levels in recent sediments that coincide with the timing of hydrocarbon drilling and production. This is supported by geographical differences on a large scale that relate to proximity to hydrocarbon drilling and production. Among 243 sampling stations, we identify 73 locations exhibiting enrichment of Ba in the upper 6 of sediment. At these locations, Ba is 1.55 to 3.55 times higher than the levels that can be expected from the shale average when Ba in detrital matter is accounted for. Excess Ba is reported in sediment surface samples in areas important to fisheries like the Lofoten area and the western Barents Sea.

1. Introduction

In several parts of the world, the oil and gas industry involves large discharges of produced water, drilling mud, drill cuttings and residues into the marine environment. These discharges contain a range of hazardous substances such as heavy metals, polycyclic aromatic hydrocarbons, alkyl phenols and radionuclides, and focus has been put on their dispersal and impact on marine sediments and biota (Ahmad et al., 2021; Celis-Hernandez et al., 2018; Dowdall and Lepland, 2012; Frost et al., 2014; Lepland et al., 2000; Neff et al., 1995; Rye et al., 2014; Rye et al., 2011; Singsaas et al., 2008; Yang et al., 2015). It has been suggested that Barium (Ba) discharged during hydrocarbon drilling and production may accumulate in recent marine sediments (Celis-Hernandez et al., 2018; Lepland and Mortensen, 2008; Lepland et al., 2000). Neither barite (BaSO4) nor dissolved Ba in seawater are considered to be toxic to marine organisms (Neff, 2002b; Neff et al., 1995). However, knowledge about the Ba distribution in recent marine sediments may be used to identify areas that are affected by discharges from the oil and gas industry. This can be of great interest for the Norwegian fishing industry.

Typical concentrations of dissolved Ba^{2+} in seawater are 4–20 μg/L and its fraction of particulate Ba is usually <1 % (Neff, 2002b). Produced water has enhanced levels of several elements and inorganic ions and their levels depend on the type of rock and its geological age (Neff, 2002a). Produced water contains dissolved Ba^{2+} in concentrations that range from 100 to 2 million μg/L (Neff, 2002b). When produced water is discharged, Ba^{2+} reacts with the SO_4^{2-} in seawater and micron-sized particulate barite precipitates, which can disperse over long distances before settling on the ocean floor (Neff, 2002b). Due to the very large volumes of discharged produced water, its impact on Ba and barite distributions in marine sediments is potentially large and far reaching. Barite is also the principal component of drilling mud (around half the dry weight) (Neff, 2008). For drill cuttings, the level of Ba depend on the drilled rock but these are most important to nearfield plumes due to high density (Frost et al., 2014; Rye et al., 2006).

Ba is an alkaline earth metal common in Earth's crust (15th in abundance). It occurs in silicate minerals and typically substitutes for potassium (K) and, to some extent, for calcium (Ca). When terrestrial rocks weather into detrital particles or leach Ba into solution, Ba is carried to the oceans by riverine runoff as barite and witherite ($BaCO_3$) (Fischer and Puchelt, 1972). Detrital input from runoff has much variation that relates to rock-type variations in content of Ba, which is important to the level of Ba in the marine sediments. Sedimentation

* Corresponding author.
E-mail address: hallvard.haanes@dsa.no (H. Haanes).

https://doi.org/10.1016/j.marpolbul.2022.114478
Received 1 September 2022; Received in revised form 24 November 2022; Accepted 6 December 2022
Available online 16 December 2022

Box 1
Information about the MAREANO project and the recent marine sediment samples taken during this project.

Since 2006, the MAREANO marine mapping program has collected surface sediments and sediment cores from the Norwegian and Barents Seas. The samples are analysed for grain size distribution, major and trace metals and organic pollutants (https://mareano.no/en/maps-and-data/chemical-data). The data are freely accessible and used in this study. MAREANO sampling focuses on depositional areas where fine-grained sediments accumulate, is guided by multi-beam echo-sounding mapping, and uses primarily a multi-corer with 60 cm long and 10 cm diameter PVC-tubes, or alternatively, a box corer. From these, either whole cores or only the top slice / surface sediment was sampled. Cores are typically 30 cm long and are cut into 1 cm slices. Samples are stored frozen, and then freeze-dried before being split for grain size analysis, total carbon (TC), total sulphur (TS) and total organic carbon (TOC) analysis, and assessment of major and trace metals (Knies et.al., 2006). Grain size is assessed through laser diffraction (Xu, 2000), with respect to percent volume assuming uniform density of the sample and divided into clay (<2 μm), silt (2–63 μm), sand (63–2000 μm) and gravel (>2000 μm) according to Geological Survey of Norway standards (Bøe et al., 2010). Geochemical analyses are done with 1 g of freeze-dried homogenised sediment using chemical extraction (7 M HNO_3 treatment in autoclave, NS-4770) with a Perkin Elmer ICP-AES/ICP-OES. Metal concentrations are reported for sediment dry weight (mg kg^{-1} dw). Ba analysis has an analytical accuracy of ±25 % and a lower detection limit of 1.0 mg kg^{-1} sediment. Al analysis has an accuracy of ±20 % and a lower detection limit of 20 mg kg^{-1} sediment. Li analysis has an accuracy of ±20 % and a lower detection limit of 0.5 mg kg^{-1} sediment.

regimes vary between marine areas depending on proximity to sediment sources, depth, and current regimes (Brown et al., 1995a, 1995b), affecting the compositional and size characteristics of accumulating sediment.

To account for detrital Ba in sediments, data can be normalised by calculating an enrichment factor (EF) based on a detrital-specific element such as aluminium (Al). Excess Ba (levels higher than expected) in recent marine sediments may thus reflect discharges from offshore hydrocarbon drilling and production and could be used to map the impact of these. This methodology has been used for Skagerrak (Lepland et al., 2000).

Ba solubility, and thus dissolved Ba concentration increases sharply with sediment depth as barite becomes unstable within the diagenetic sulphate reduction zone. Ba dissolved in interstitial water deep in sediments coming up through hydrothermal vents or cold seeps can cause barite precipitation and the formation of barite nodules in upper sediment layers or on the seabed surface (Griffith and Paytan, 2012). Sediments adjacent to vent and seep localities may locally have high Ba levels and will stand out as outliers when assessing the distribution of Ba among samples across large areas.

In this study, we assess Ba levels in recent marine sediments in the Norwegian and Barents Seas and compare with co-variation in parameters related to sedimentation and regional geology. We use data from the Norwegian MAREANO database (Box 1) to assess spatial and temporal variations in Ba levels, and to identify Ba enrichment in certain geographic areas. Our objective is to assess whether Ba levels have increased due to discharges from the oil and gas industry while accounting for Ba related to detrital material and sedimentation-related parameters.

2. Study area and geology

The study area consists of the Barents and Norwegian Seas, which are bordered by Norway, Russia and Svalbard in the south, east and north, respectively. To the south lies the North Sea. The main direction of the ocean currents in these waters is northbound (Fig. 1).

The Norwegian oil and gas industry started in the late 1960s, with activity dominating in the North Sea until today but expanding into the Norwegian and Barents Seas in the past decades (Fig. 1). Information about installations and production over time is given by the Norwegian Petroleum Directorate. The total oil production per area at the end of year 2021 was, for the North, Norwegian and Barents Seas, 3970, 645 and 16 million cubic meters of oil, respectively (https://www.norskpetroleum.no/en/facts/historical-production/). Also, the British, Dutch, and Danish oil and gas industries are large in the North Sea (https://www.ospar.org/work-areas/oic) and commenced in the same time period. Vast areas of the seafloor may be impacted. Given the northbound direction of the ocean currents, areas in the Norwegian and Barents Seas may also be impacted. This is of concern to the Norwegian fishing industry.

The Barents Sea is a relatively shallow (typically <400 m) marginal sea with both non-deposition shallows and deeper areas with sedimentation (Vorren et al., 1991). The Norwegian Sea comprises both continental margin, slope and abyssal waters. Here, sedimentation takes place primarily on the continental slope and the deeper parts of the 100–500 m deep and 45–230 km wide shelf, being most narrow in the north outside Lofoten and Troms (Thorsnes et al., 2016). To the west, the continental slope of the Norwegian-Barents-Spitsbergen continental margin comprises an up to 3 km thick glacial sediment layer characterised by submarine slides, large-scale mass wasting and smaller seafloor features (pockmarks, mud volcanos and diapirs) produced by mobilised fluids and sediments (Damm and Budéus, 2003; Hjelstuen et al., 1999). Examples are piercing mud diapirs and the Håkon Mosby mud volcano (72.0 N, 14.7 E) north of Norway at 1250 m depth, which is a prominent deep-sourced, fluid flow feature at the continental slope (Milkov, 2000; Vogt et al., 1997). It has a 50–100 m high plume shaped by thermal convection and vertical and horizontal turbulent diffusion (Damm and Budéus, 2003; Egorov et al., 1999). At the continental slope of the Norwegian Sea just south of Lofoten, the Vøring plateau and basin also contains piercing mud diapirs and probably a mud volcano (Hjelstuen et al., 1997; Hovland et al., 1998).

Sediment provenance in the Norwegian and Barents Seas includes crystalline basement and sedimentary rocks. Ba concentrations vary greatly among different magmatic rocks, ranging from 5 mg kg^{-1} in ultramafic rocks to >600 mg kg^{-1} in granitic rocks. Sedimentary rocks, which are prominent in the Barents Sea, have Ba concentrations ranging from 90 mg kg^{-1} (limestone) to 550 mg kg^{-1} (shale) (Reimann et al., 1998). Sedimentation rates in the Norwegian and Barents Seas in recent times are generally in the range of 0.5–2 mm $year^{-1}$ (Heldal et al., 2002; Jensen and Bellec, 2021; Maiti et al., 2010; Smith et al., 1995; Zaborska et al., 2008).

3. Materials and methods

3.1. Data and parameters

Results from 243 open sea stations (sampled from 2003 to 2017) were downloaded from the MAREANO data base, consisting of 127

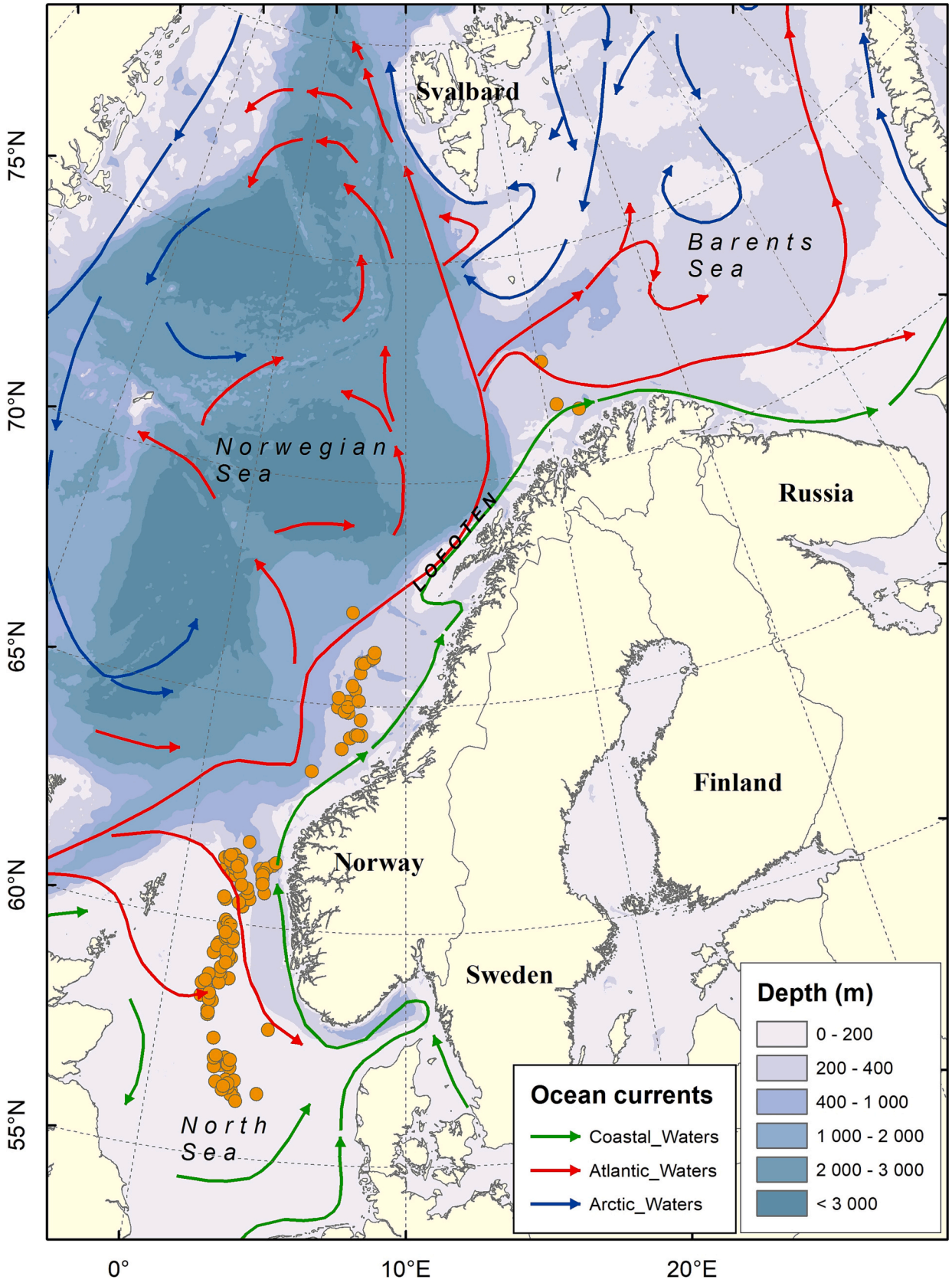

Fig. 1. Overview of Norwegian oil and gas fields. Data source https://www.norskpetroleum.no/en/facts/field/ and https://www.npd.no/en/about-us/open-data/.

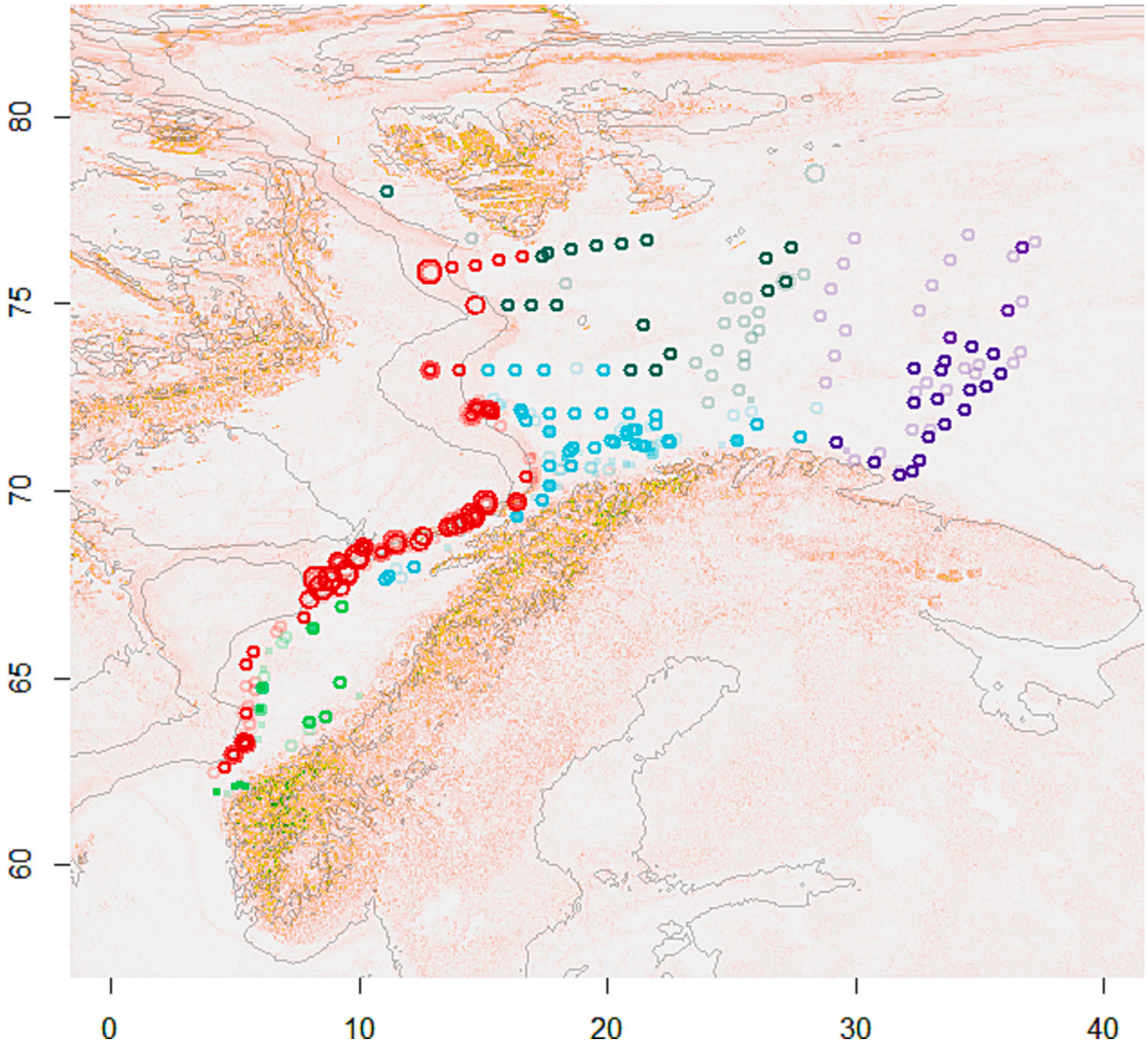

Fig. 2. All studied samples categorised according to area; with the Norwegian Sea south in green, the continental slope in red, the Barents Sea south-west and Norwegian Sea north in light blue, the Barents Sea north and central in green, and the Barents Sea south-east in purple. Relative differences in Ba content given by the size of points (0.5 cex per SD). Different numbers of samples at one point gives different colour intensities with stronger colours for more samples. Axis with longitudes (X) and latitudes (Y). (For interpretation of the references to colour in this figure legend, the reader is referred to the web version of this article.)

Table 1
Range (min, max), mean and standard deviation (SD) for the content (mg kg^{-1}) of barium (Ba), aluminium (Al) and lithium (Li) and the percent of size fractions clay (<2 μm) and silt (2–63 μm) among all studied samples, as well as the range of intra-core mean and SD.

	Min	Max	Mean	SD	Intra-core mean range	Intra-core SD range
Ba	10	401	138	82	[18, 339]	[2, 80]
Al	2200	28,600	16,448	5119	[3564, 25,571]	[133, 8991]
Li	3	49	25	9	[4, 45]	[0, 15]
% clay	0	15	8	3	[2,13]	[0, 4]
% silt	0	90	63	19	[12, 88]	[1, 25]

sediment surface samples (either 0–1 or 0–2 cm) and 136 sediment cores divided into a total of 2553 slices (totally n = 2680 sediment samples). Surface samples are the top slice of cores where the rest of the core was discarded. Moreover, MAREANO data are typically from depositional areas of sediment and involve elaborate geochemical analyses (see Box 1). All sampling stations are at distance from oil and gas installations. The number of slices per core varies from 5 to 42 (mean: 22, SD: 7.7). We assess spatiotemporal variations in sediment Ba concentrations. Variations with core depth are used to assess changes over time, like before and after the onset of the oil and gas industry.

Sediment slices are grouped into three depth intervals; upper: [0, 6 > cm, middle: [6, 16] cm and lower: <16, 48] cm. Locations with only upper slices are included to assess spatial variations. Assuming sedimentation rates of <1 mm $year^{-1}$ (see study area section), most impacts of the oil and gas industry will be expected in the upper depth interval while diagenetic influence on barite stability can be expected in the

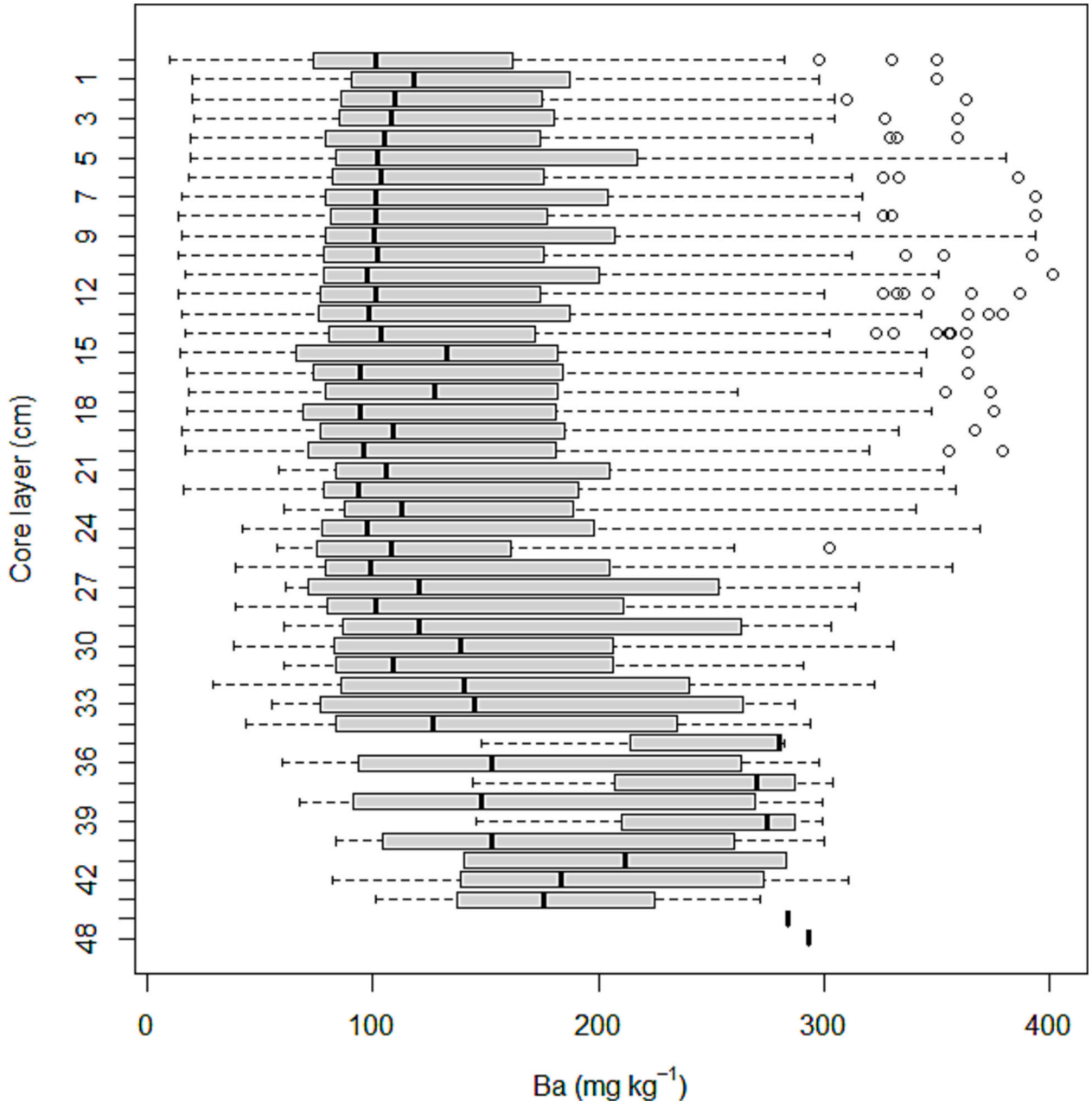

Fig. 3. Boxplots of Ba content among core slices with increasing core depth (75 percentile box with median as bold line, end of boxes 25 and 75 percentile, whiskers 95 confidence interval and outliers as dots).

lower depth interval. All studied samples are categorised into five spatially defined areas (Fig. 2): NS: Norwegian Sea south (Tertiary sedimentary bedrock), CS: continental slope (deep areas marginal to continental shelf), BSW: Barents Sea south-west and a part of Norwegian Sea north (Tertiary sedimentary bedrock), BSC: Barents Sea north and central (Jurassic to Tertiary sedimentary bedrock), and BSE: Barents Sea south-east (Triassic to Permian sedimentary bedrock). Since water masses in the area (Norwegian coastal water and Atlantic water) flow towards the north, latitude per sample is included as a potential explanatory variable. To assess co-variation with grain size, we include the clay and silt fractions in the analyses. Aluminium (Al) and lithium (Li) are assumed to correlate with detrital fine- grained sediments and are used as a proxies for the grain size variations, i. e. mainly clay size fraction (Loring and Rantala, 1992).

3.2. Enrichment factor

To assess whether Ba is in excess requires knowledge about the natural/geogenic distribution in sediments. This can be used to scale samples (normalization) to account for the detrital part of sediments. For sedimentary deposits, Al can be considered indicative of the detrital aluminosilicate fraction (Tribovillard et al., 2006). The Ba/Al ratio can thus be used to normalise scaling (Reitz et al., 2004). This approach has been used earlier in the North Sea (Lepland et al., 2000). Here, we follow Tribovillard et al. (2006) and calculate the Enrichment Factor (EF) as:

$$EF = \left(Ba_{sample}/Al_{sample}\right)/\left(Ba_{average\ shale}/Al_{average\ shale}\right)$$

The Ba EF expresses whether the sample concentration of Ba is in excess compared to the average in shale when the value is greater than one (Tribovillard et al., 2006). We use literature values for upper crust

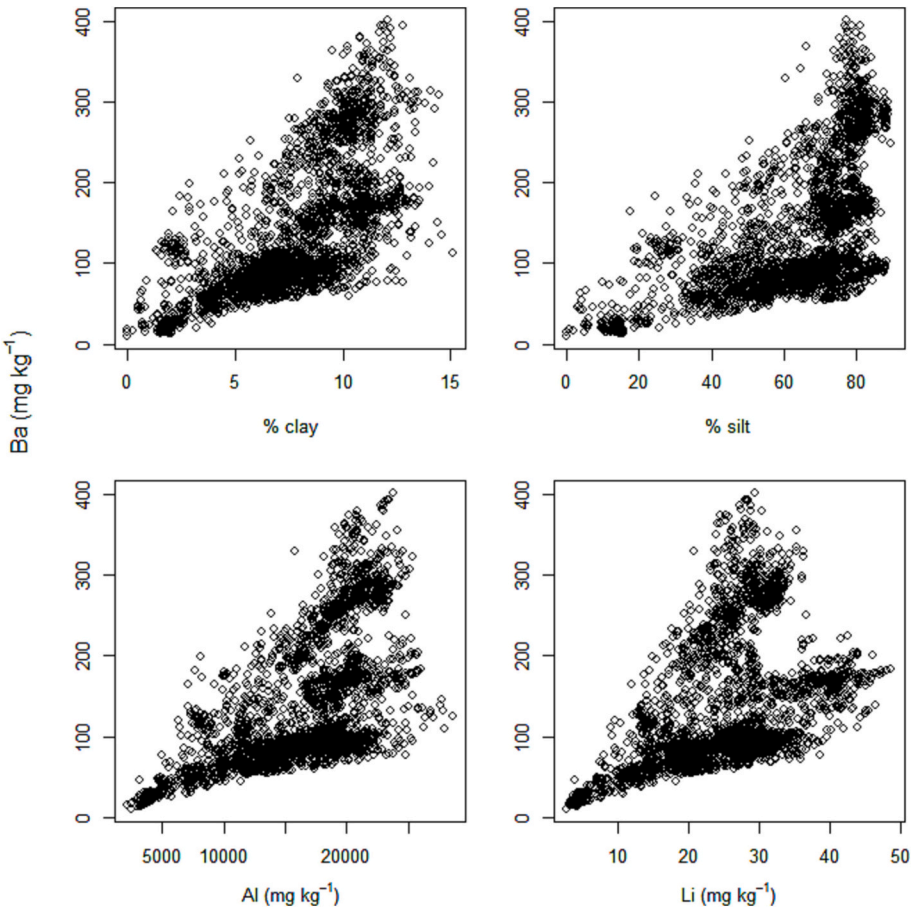

Fig. 4. Plots of Ba content in all studied samples against contents of percent clay (% clay) and silt (% silt), aluminium (Al) and lithium (Li).

averages of Ba (550 mg kg^{-1}) and Al (80,400 mg kg^{-1}) (Tribovillard et al., 2006) and calculate the enrichment factor EF for all samples for which Al and Ba are measured. Note, Al is not affected by diagenetic processes in marine sediments (Loring and Rantala, 1992). Samples with excess Ba in the upper parts of sediments are identified (age less than the oil and gas industry), providing a suggestion for areas impacted by hydrocarbon drilling and production.

3.3. Analyses and statistical models

Correlation analyses and statistics are done in R (R Core Team, 2016).

One linear model has Ba concentration as the response variable, and clay, silt, Li, Al, geographic area and water depth as predictor variables. To address differences from one geographic area to the next, we use reverse Helmert contrasts (called Helmert in contrasts package R), which compares each new level with the mean of previous levels.

Another linear model has Ba EF as the response variable and the same predictor variables and contrasts. It is used to predict the expected Ba EF of each sample from the observed values in the predictor variables (using the fitted function in R). This is done to identify samples deviating from what the model predicts. Such samples may have a moderate and not outstanding Ba EF value that with the values of the predictor variables should have had a much lower Ba EF value. Such samples are otherwise hard to identify. To do so, the observed Ba EF of each sample is subtracted from the value predicted (expected) by the model and all resulting values larger than one standard deviation are identified. Samples yielding a Ba EF larger than one plus one standard deviation and samples with a larger observed Ba EF than statistically predicted, are used to identify areas with excess Ba.

3.4. Maps

Maps are made in R (R Core Team, 2016) using packages sp., rgdal, raster, rgeos and sf (Bivand et al., 2019; Bivand and Rundel, 2012; Hijmans and van Etten, 2012; Pebesma, 2018; Pebesma and Bivand, 2005) and bathymetry is from a gif-file background from GEBCO Compilation Group (2022) GEBCO_2022 Grid (doi:https://doi.org/10.5285/e0f0bb80-ab44-2739-e053-6c86abc0289c). One map is made of all sampling localities, grouped by colour according to geology and sized according to Ba content. Another map is made showing only samples with Ba EF one standard deviation larger than statistically predicted Ba content.

4. Results

Barium concentrations in recent marine sediment in this study range from 10 to 401 mg kg^{-1} dw, except in one anomalously Ba-rich station

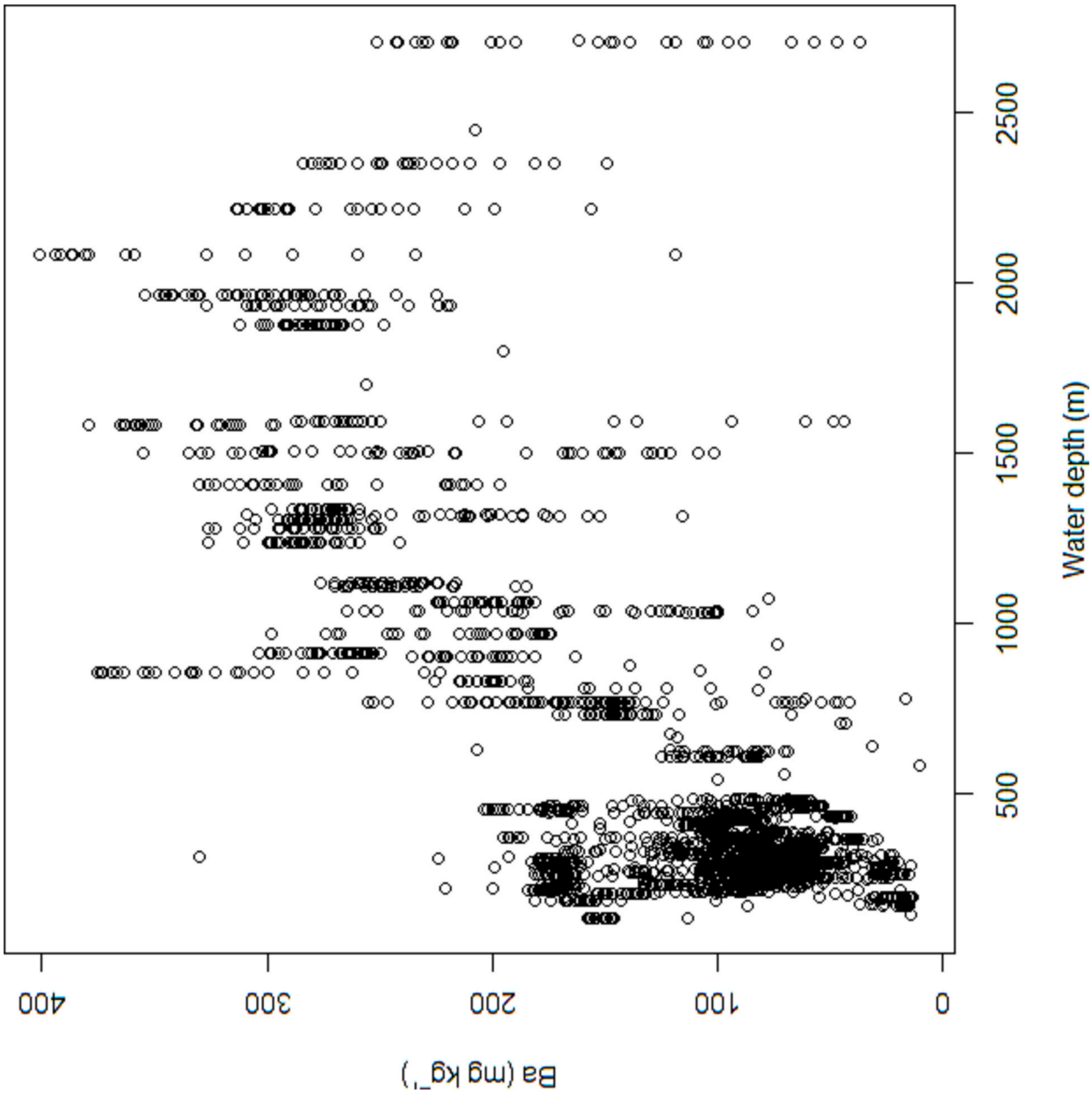

Fig. 5. Plot of Ba content in all studied samples of sediment with water depth of sampling stations.

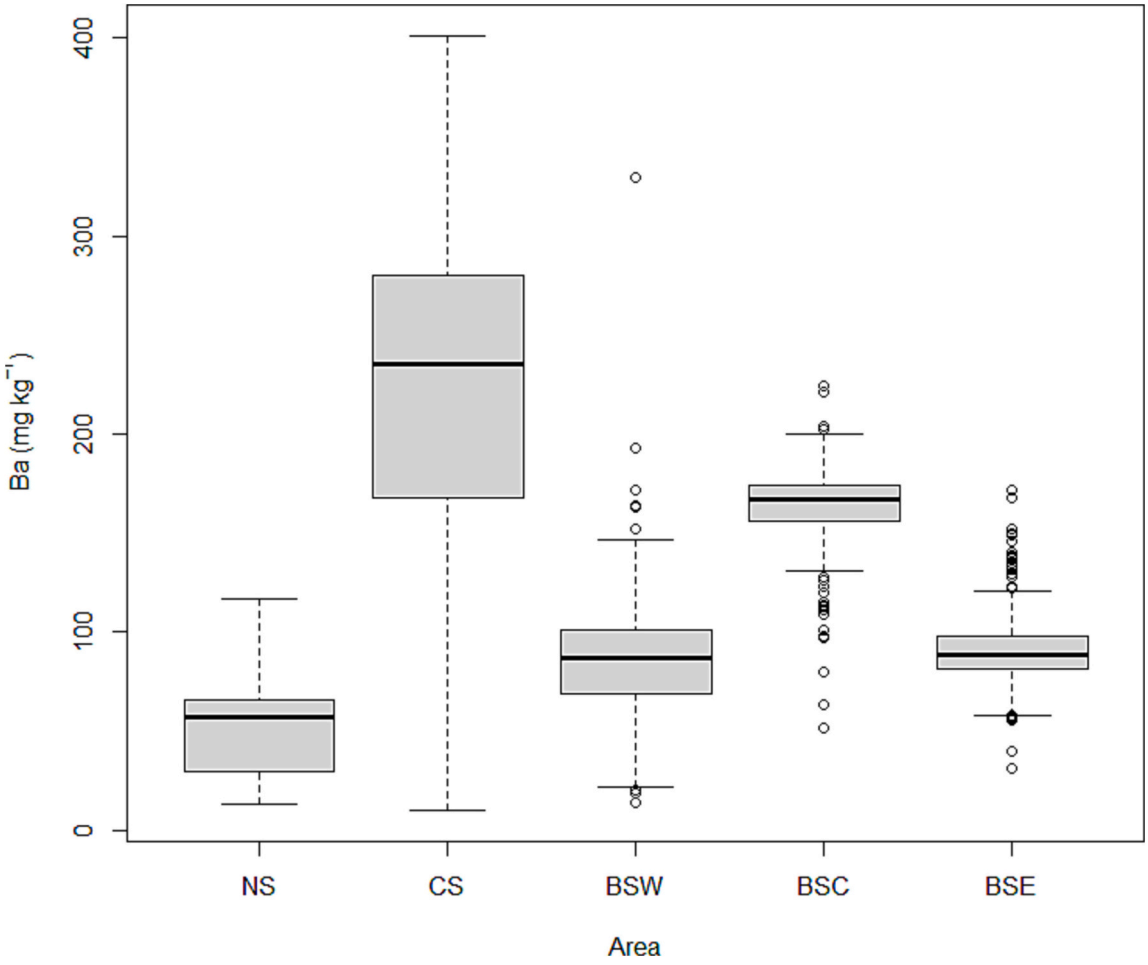

Fig. 6. Boxplot of Ba concentration in all studied samples from different areas. NS: Norwegian Sea south, CS: continental slope, BSW: Barents Sea south-west and Norwegian Sea north, BSC: Barents Sea north and central, and BSE: Barents Sea south-east.

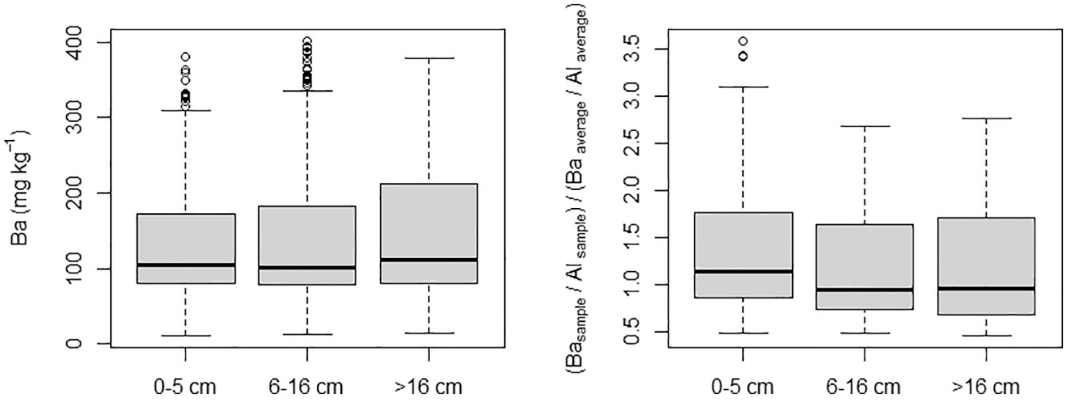

Fig. 7. Boxplots of Ba concentration (left) and Ba enrichment factor (right) in studied sediment samples within groups of core slice depths.

(1090 mg kg^{-1} dw). This is located close to the Håkon Mosby mud volcano in the south-west Barents Sea (Knies et al., 2006) and is excluded from further analyses. There are large variations in levels of Ba, Al, Li and grain size among samples (Table 1). Most parameter distributions are near symmetrical (not in need of transformation).

Ba concentrations are higher in the deepest sediment core slices, but several cores also have outlier values in slices closer to the sediment surface (Fig. 3). The content of Ba in each slice is positively correlated to clay ($r = 0.68$, $p << 0.001$), silt ($r = 0.57$, $p << 0.001$), Al ($r = 0.59$, $p << 0.001$) and Li ($r = 0.44$, $p << 0.001$), especially when levels are low (Fig. 4). There is a strong correlation between Ba content and water depth ($r = 0.73$, $p << 0.001$), even though there is much variation (Fig. 5). The correlations between Ba content and clay, silt and water depth, respectively, are as expected since these parameters are related to sedimentation regime. As expected, there are large differences in Ba sediment concentrations between the different areas sampled (Fig. 6). Levels of Ba seem to increase towards the north and are highest on the continental slope. There are, however, large variations (Figs. 2, 6).

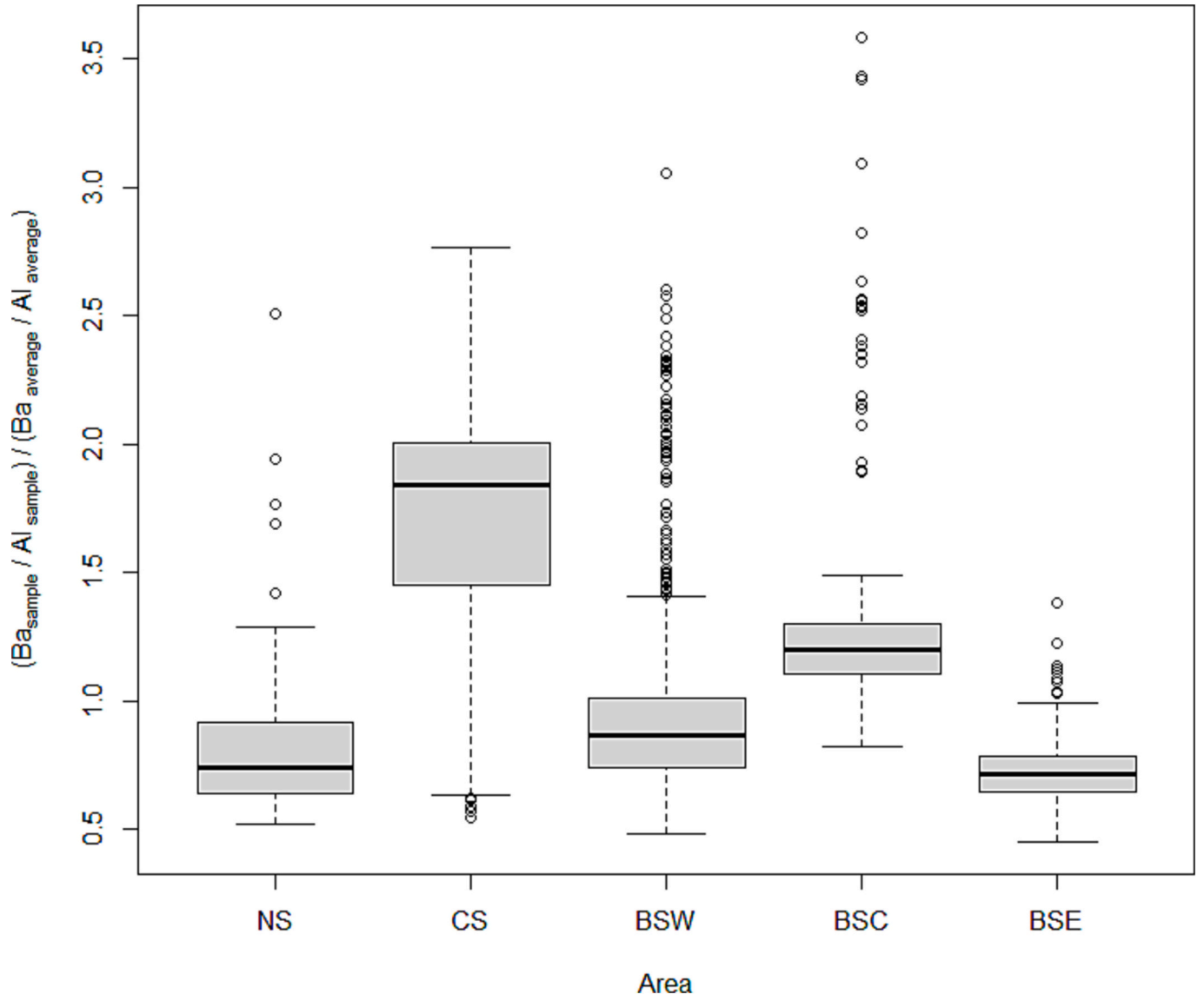

Fig. 8. Boxplot of Ba enrichment factor in sediment samples in different areas. NS: Norwegian Sea south, CS: continental slope, BSW: Barents Sea south-west and Norwegian Sea north, BSC: Barents Sea north and central, and BSE: Barents Sea south-east.

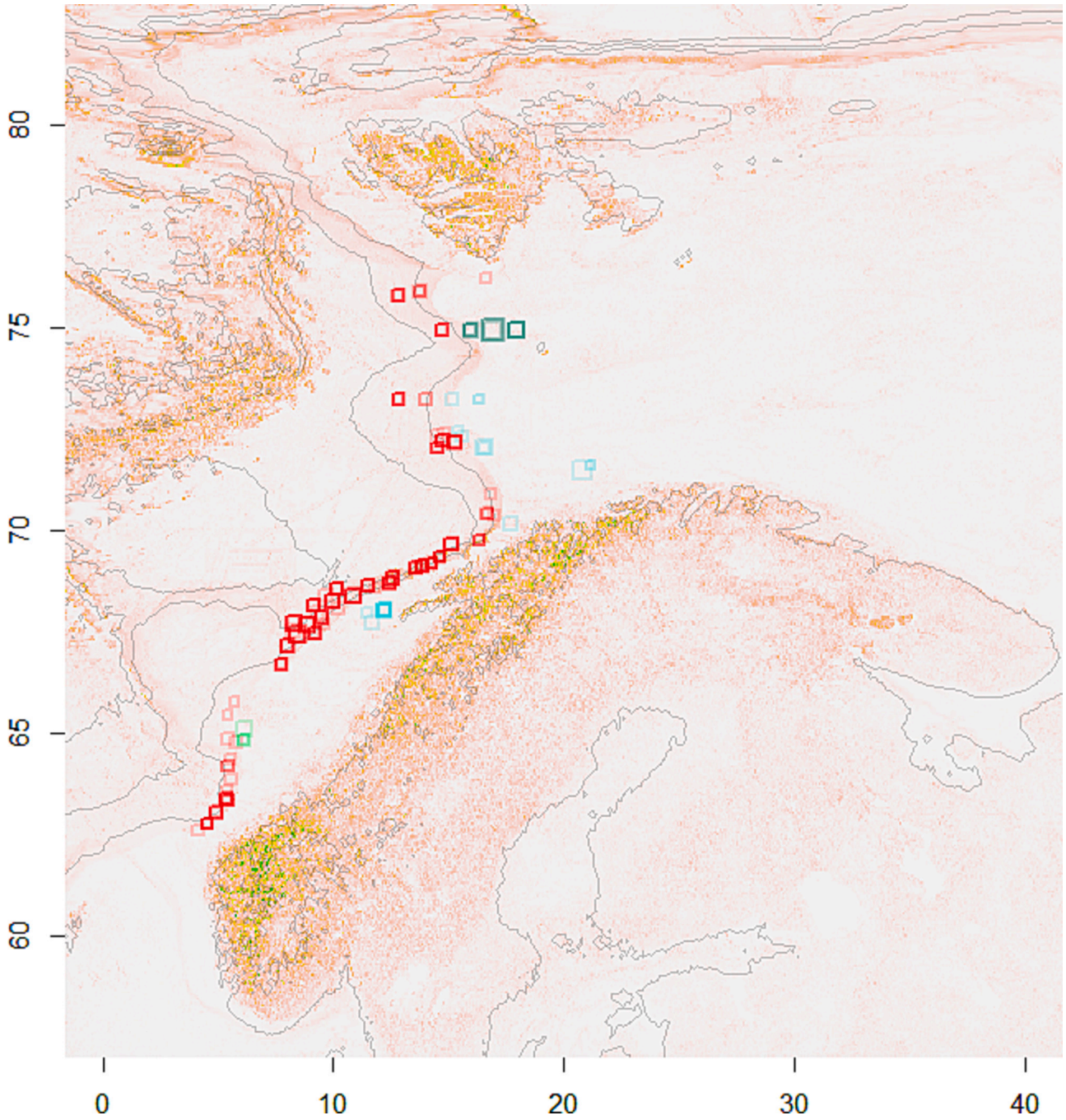

Fig. 9. Locations of studied sediment samples (squares) with Ba enrichment factor (EF) larger than one standard deviation (0.55) from the assumption of no enrichment (EF = 1), with cex is equal to EF/2. Samples from different areas are indicated by colours with the Norwegian Sea south in green, the continental Slope in red, the Barents Sea south-west and Norwegian Sea north in light blue, and the Barents Sea north and central in green. Different numbers of samples at one point gives different colour intensities. Decimal degrees on axis for longitudes (X) and latitudes (Y). (For interpretation of the references to colour in this figure legend, the reader is referred to the web version of this article.)

4.1. Ba excess compared to shale average

Among all studied samples, the Ba enrichment factor (EF) ranges from a minimum of 0.45 to a maximum of 3.58 (mean: 1.21, SD: 0.55) with values >1 expressing excess Ba compared to shale averages when accounting for Al in the detrital aluminosilicate fraction. Among the three depth intervals, the Ba EF is highest in the upper interval (Fig. 7). The relationship of the Ba EF to predictor variables is only weakly correlated with clay ($r = 0.27$, $p << 0.001$), silt ($r = 0.14$, $p << 0.001$) and Al ($r = 0.11$, $p << 0.001$), and has no correlation with Li ($p > 0.86$) but with water depth ($r = -0.67$, $p << 0.001$). For the Ba EF, the differences between the area categories are unchanged, with most of the highest values on the continental slope but many outlier values in the areas BSW (Norwegian Sea north and Barents Sea south-west) and BSC (Barents Sea north and central, which are both otherwise dominated by lower values (Fig. 8). Ba EF shows a bimodal distribution, with a main distribution centred around 1 and a standard deviation (SD) of 0.55, and a second around 2 with a wider dispersion. The latter dispersion is probably due to an additional Ba source. This is supported by these samples having a Ba EF >1.55 (i.e., more than one SD away from the first distribution and outside a 95 % confidence interval given one SD in each direction of 1) and by them being numerous (741 samples and 73 cores).

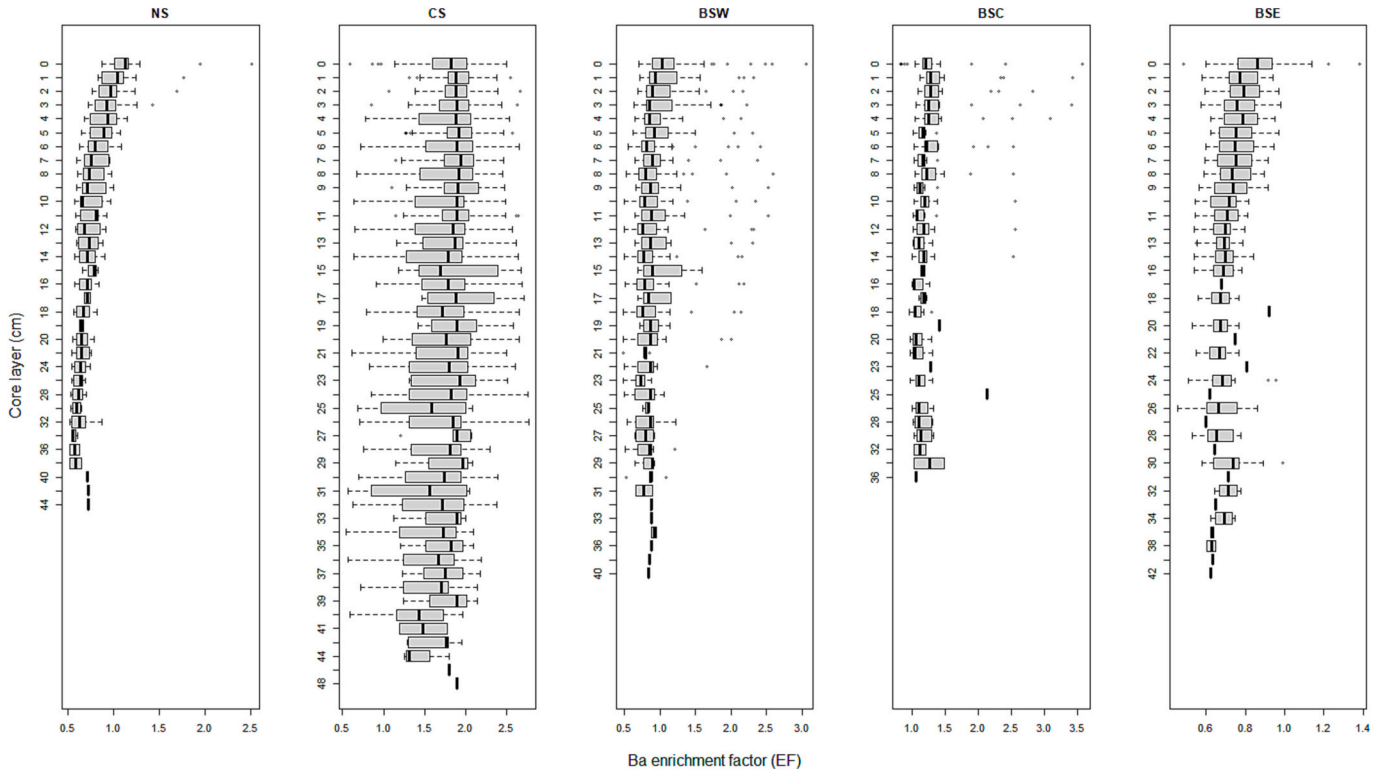

Fig. 10. Boxplots of Ba enrichment factor (EF) for sediment samples from the five assessed areas given for increasing sediment depth (75 percentile box with median as bold line, end of boxes 25 and 75 percentiles, whiskers 95 confidence interval and outliers as dots). Note the different scales on the Ba EF x-axes.

Among these, 252 samples are in the top 6 cm, and these are subdivided between 24 surface sediment samples and 228 core slices in 49 cores (total of 73 locations). These are found along the continental slope, as well as in the Norwegian Sea and the southwestern Barents Sea (Fig. 9). However, the number of outliers and patterns of Ba EF with increasing sediment depths vary between areas (Fig. 10). A typical core for the southern Norwegian Sea with Ba excess in upper parts is given in Fig. 11. Examples of differences to other areas are seen in three other example core profiles (Figs. 12-14), of which one is near the Håkon Mosby mud volcano.

4.2. Statistical models

The statistical model of Ba verifies expected relationships. The relationship between Ba concentrations in samples and variation in predictor variables are established in a linear model and are increasing as expected except for a decreasing trend with Li (Table 2). All terms in the model are significant except percentage of clay. The Helmert contrasts show significant differences between areas, as can also be seen in Fig. 6. Controlling for variation in all terms, use of Helmert contrasts show significant differences in Ba level from area to area with an increase from the Norwegian Sea (NS) to the continental slope (CS); a decrease from CS to western Barents Sea (BSW); an increase from BSW to the central Barents Sea (BSC); and a decrease from BSC to the eastern Barents Sea. The same model with normal control/treatment contrasts shows that all areas have higher levels than NS, except BSE. Also, notice the much larger effect sizes of the area and Li terms, as well as the different directions of terms (Table 2).

When the same statistical model is run for Ba EF with the same terms, somewhat less variation is explained by the predictor variables (Table 3). This suggests that the model can be used for statistical prediction to identify samples deviating in Ba EF given the values of predictor variables in each sample. For this model the clay term is near significant while significance is lost in the latitude term and the Al term (as expected due to Al standardization). Direction and relationships of the terms with this model are also similar to those of the Ba model, and with control/treatment contrasts, all areas have significantly higher Ba EF than the Norwegian Sea. However, both statistical models (Ba and Ba-EF) have deviations from normality in residuals, suggesting explanatory factors or synergies might be missing.

4.3. Excess Ba according to predictor variables and statistical model

The statistical model predicts the Ba EF expected for each sample. Subtracting this from the observed Ba EF to obtain a sample EF delta value gives a symmetrical distribution around zero, as expected. Among all studied samples with a Ba EF value more than one SD (EF = 0.55) larger than predicted from the statistical model, 44 samples are among slices shallower than 6 cm while 77 are among deeper slices. These samples are so far from the centre of the distribution that they most likely are heavily influenced by an additional source of Ba.Among all studied samples with a Ba EF value more than one SD larger than predicted from the statistical model (i.e., falling outside the 95 % confidence interval (CI) considering one SD in each direction), 14 samples are from strata shallower than 6 cm and 14 samples are from deeper strata. These are found at the continental slope, in the Norwegian Sea and in the western Barents Sea (Fig. 17).

5. Discussion

This study shows differences in Ba in recent marine sediments between different areas along the Norwegian continental margin (Figs. 6, 11), partly related to proximity to hydrocarbon drilling and production sites, when all explanatory variables are controlled for (Table 2). Compared to the location of these sites in Norwegian waters (Fig. 1), the locations with high concentration of Ba (Fig. 2) and the locations identified with significantly enriched Ba (Ba EF > 1.55, Fig. 9) seem to correspond well. Apparently, the continental slope, Norwegian Sea and

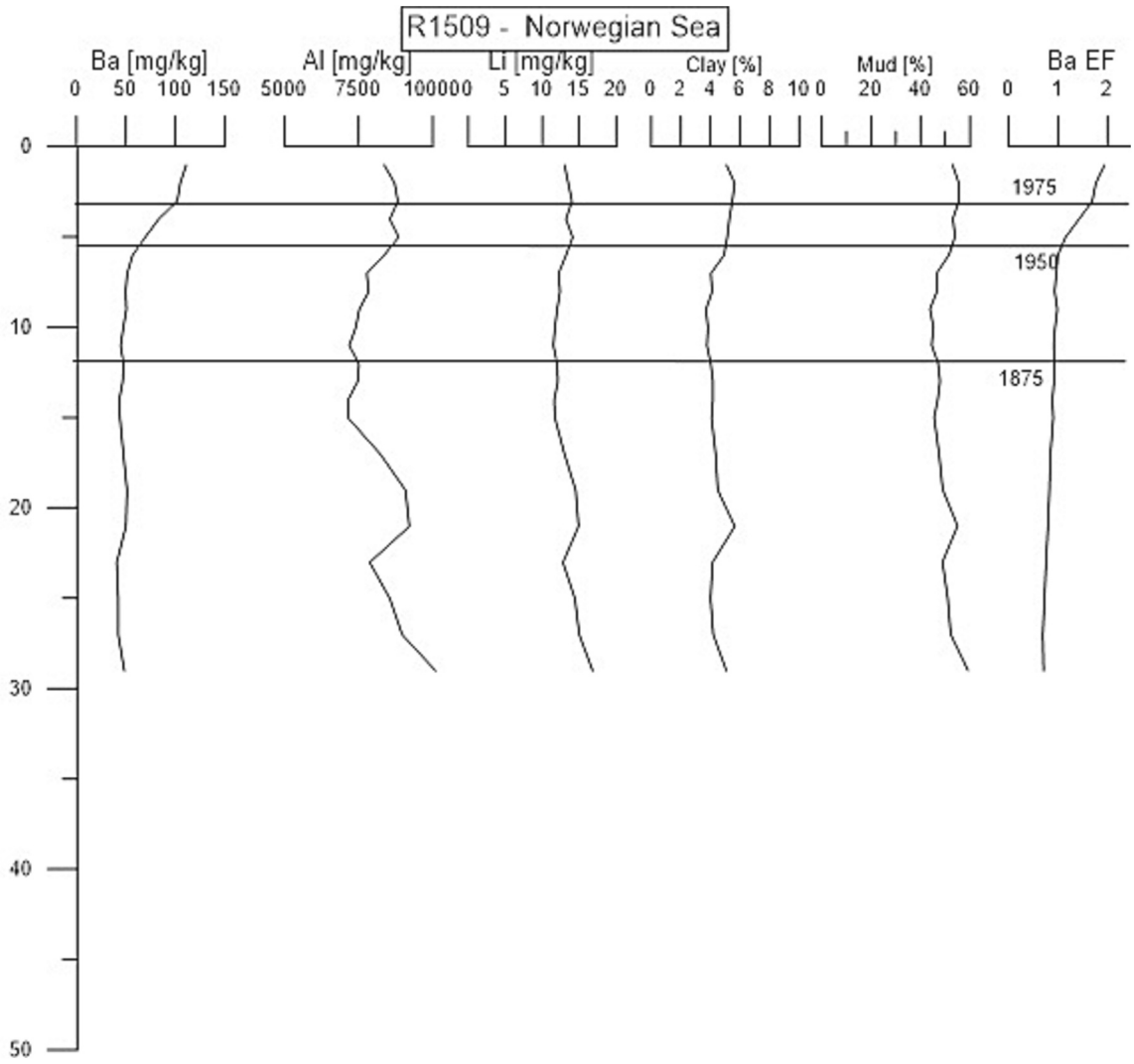

Fig. 11. ^{210}Pb-dated sediment core (R1509) from southern part of the Norwegian Sea. Ages are marked as lines at three depths. Parameters include Ba, Al, Li, clay content, mud content and barium enrichment factor (EF). Note marked increase in barium concentration and enrichment factor at the top of the sediment core.

southwestern Barents Sea stand out (Figs. 8, 9 and exemplified in Figs. 11-16). Natural sources of Ba are, however, also notable, like the cluster with enhanced Ba EF values north of Norway near the Håkon Mosby mud volcano (72.0 N, 14.733 E), and as shown in the example core from Håkon Mosby mud volcano (Fig. 13). The mud diapirs and volcano in the Vøring plateau and basin (Hjelstuen et al., 1997; Hovland et al., 1998) may thus explain higher Ba EF levels at the continental slope (Figs. 8-9), where the upper parts of sediment do not stand out as much (Fig. 10 and exemplified in Fig. 12). Note, however, that then explanatory variables are not taken into account. Moreover, the shallow areas of the North Sea have little sedimentation, and fine-grained particles and organic matter are transported to the Norwegian trench, Norwegian Sea and continental slope (de Haas et al., 1997). This could also explain why in the statistical models for both Ba and Ba EF, among explanatory parameters, the area differences are the largest (Tables 2 & 3) and Ba concentration and enrichment is highest at the continental slope. In both models there is a significant positive relation to water depth. In general, the amount and size distribution of detrital material reaching sediment depends on the sedimentation regime, which depends on current velocity, turbidity, and water depth (Brown et al., 1995a, 1995b; de Haas et al., 1997; Zaborska et al., 2008). This explains the significance of terms in the statistical models associated with sedimentation regime.

Overall, there are large variations in Ba concentrations and enrichment in the upper 6 cm both within and among areas (Fig. 7). Both the Ba and Ba EF models show significance in most terms, including a negative trend with increasing sediment depth (Tables 2, 3). In other words, the results indicate an increase in Ba levels and enrichment in recent times, that coincides with the onset of the oil and gas industry. In the Ba model, the Li and the Al terms are significant, as expected from their correlation with sedimentation regime and relation to grain size, while the Al term is not significant in the Ba EF model, as expected after normalising for sample Al content. Also, related to sedimentation regime, the silt term is significant and positively correlated in both models to Ba and Ba EF, while the clay term is not near significant in the Ba model but close to significant in the Ba EF model (Tables 2 and 3). This may relate to differences in sedimentation rates. By comparison, for the Ba EF, the area pattern is even clearer with less variation within each area with the exception of high outliers in the western and central Barents Sea (Fig. 8, Tables 2, 3).

An alternative explanation to enrichment of Ba in recent sediments could be increased diagenetic recycling within the sediments causing enrichment of barite in the top-slice sediments, although it seems unlikely that this would be significant under well-oxygenated, bottom water conditions. Moreover, in the statistical model for Ba EF, when accounting for covariation with explanatory variables, the sediment depth term is significant and negative (Table 3), supporting an increase in sediment Ba in recent decades. Also, a few samples stand out with

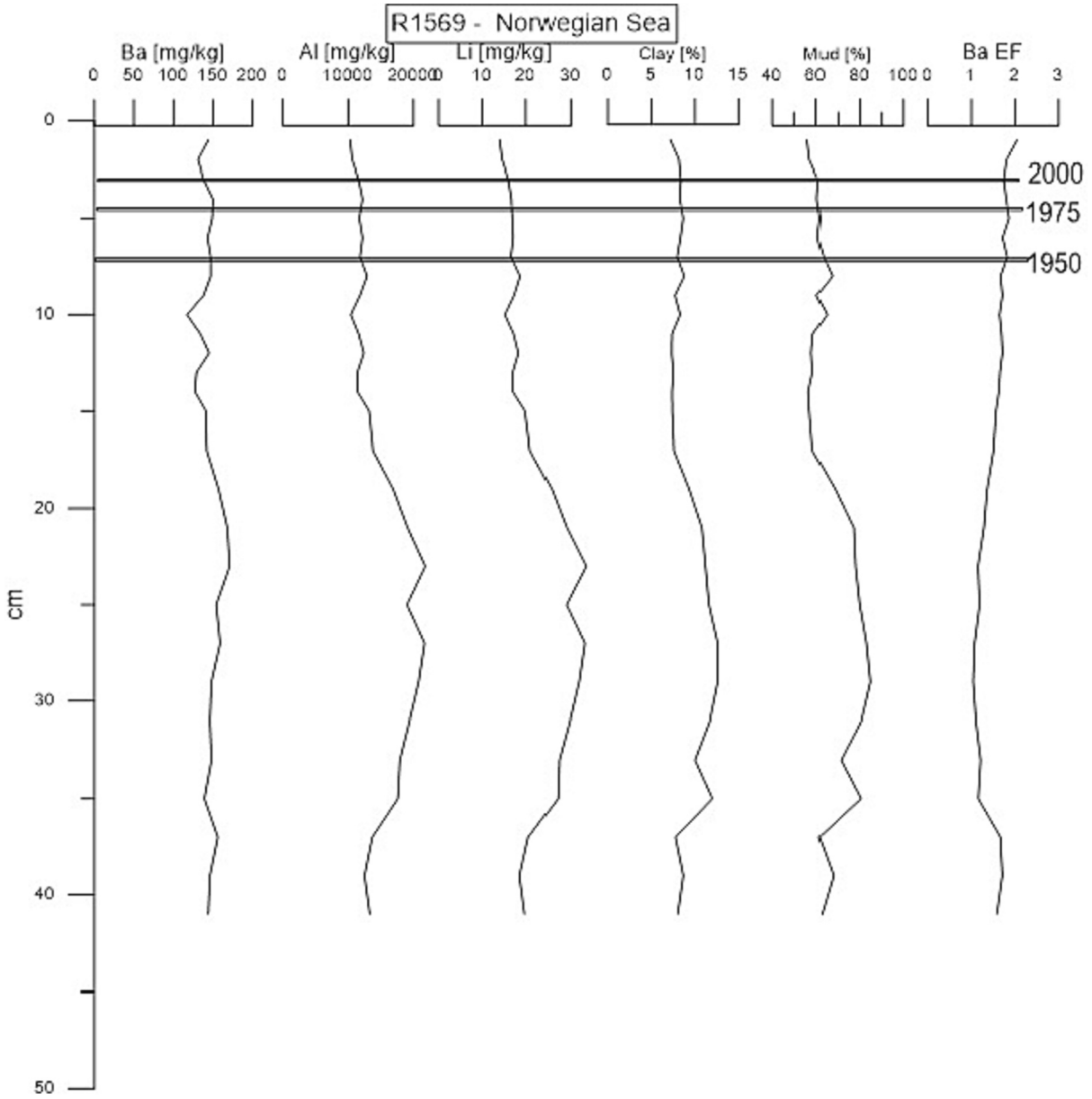

Fig. 12. ^{210}Pb-dated sediment core (R1569) from Norwegian Sea slope, showing Ba, Al, Li, clay content, mud-content and Ba enrichment factor (Ba EF). Ages are marked as lines at three depths. No significant changes are seen in Ba concentrations or Ba EF with depth.

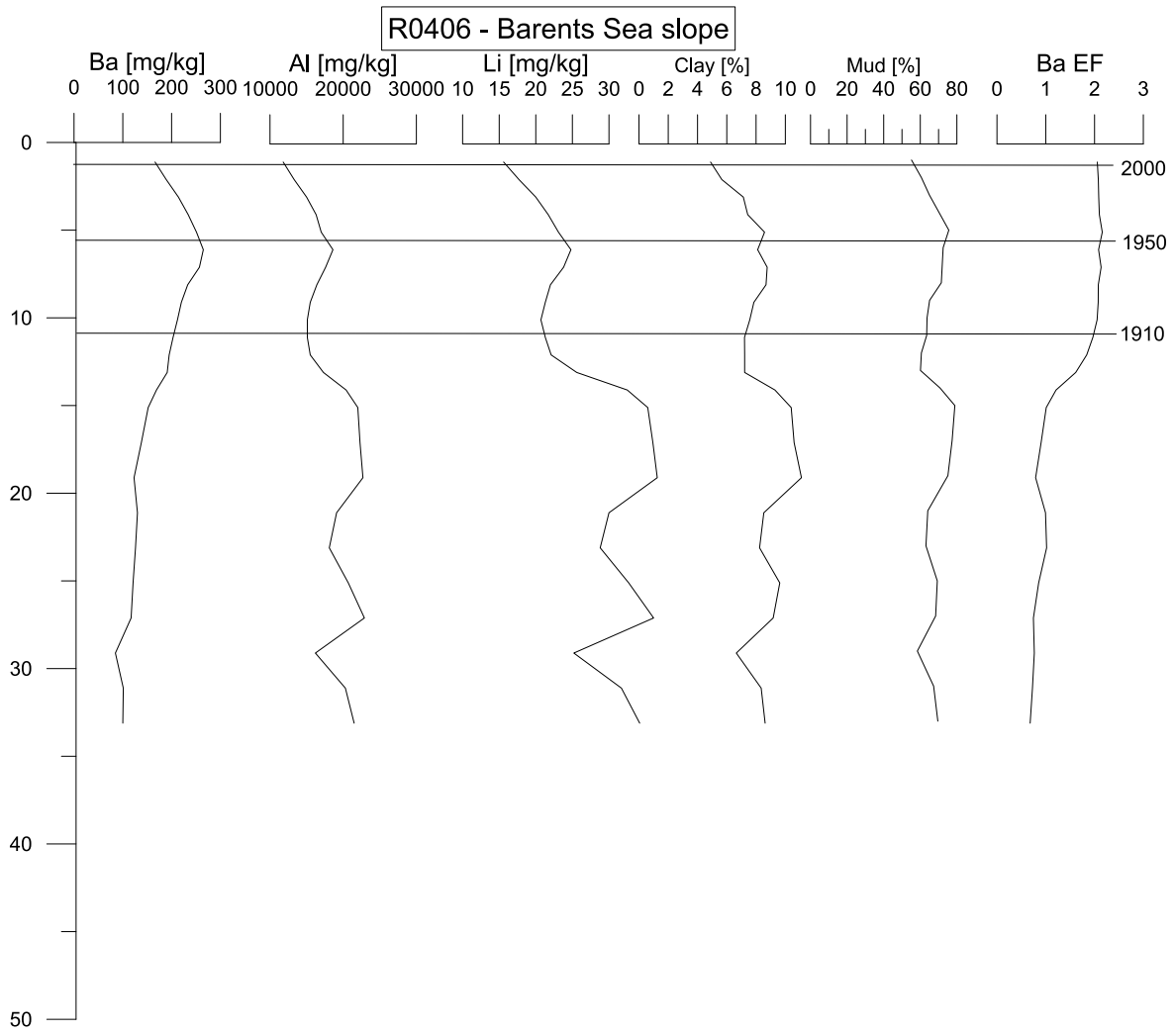

Fig. 13. ^{210}Pb-dated sediment core R0406 from Barents Sea slope. Parameters include Ba, Al, Li, clay content, mud content and barium enrichment factor (EF). Ages are marked as lines at three depths. Comment: R0406 is relatively close to the Håkon Mosby mud volcano (approx. 25 km NNE of HMMV).

higher than predicted Ba EF value given predictor variable values, and even though these Ba EF values are not high, they should have been much lower according to the statistical model prediction given the predictor variable values.

In general, Ba levels are higher in sediments derived from granitic rocks compared to mafic rocks due to elevated abundances of K-feldspars and phyllosilicates in granitic rocks. For sedimentary source rocks, clay mineral and organic matter-rich shales have considerably higher Ba concentrations compared to sandstones and sedimentary carbonate rocks. Looking at spatial Ba concentration variations in marine sediments, it is therefore important to consider and control for lithologic variations, which is why we calculated the Ba EF. EF = 1 when Ba is equal to shale Ba average.

In the Gulf of Mexico, where there is a clear impact of the oil and gas industry, a minor increase has been found for Ba EF (<1.5) in upper sediment layers (Celis-Hernandez et al., 2018). In contrast, surface sediments collected close to oil and gas platforms in the Beibu Gulf of China have Ba EF values up to 76 and on average 5.4 (Yang et al., 2015). In our study, Ba EF values in the range 1.5 to 3.5 are in the majority at the continental slope and included many outliers in the northern Norwegian Sea and south-west Barents Sea, several in the north and central Barents Sea and some in the southern Norwegian Sea (Fig. 8). Also, in some of the assessed areas, Ba EF values larger than one standard deviation (SD) higher than EF = 1 are found in numerous surface sediment samples (Fig. 9). This applies to the continental slope, Norwegian Sea and western Barents Sea; areas located downstream of the North Sea with extensive hydrocarbon drilling and production activities. Looking at samples with a Ba EF value more than one SD larger than statistically predicted, these are much fewer but appear in the same areas (Fig. 17). One reason why only a few such locations are identified may be the large portion of the samples having a Ba EF value larger than one (but less than one SD larger than one) and their bias on model prediction (towards predicting too high Ba EF values). The new locations identified this way, which have a Ba EF between one and one + SD, are however, interesting, suggesting these stand out regarding variation due to the other explanatory variables. Other studies show Ba enrichment in large parts of the deep North Sea seafloor with sedimentation (Lepland et al., 2000), near (< 4 km) a hydrocarbon installation site in the Norwegian Sea in the form of sand grain-sized barite from drilling mud (Lepland and Mortensen, 2008), and in the near-field sediments of a shallow nearshore release point in the UK of produced water (Ahmad et al., 2021). This is consistent with our findings.

Both the Ba and Ba EF models suggest increased Ba levels in recent marine sediments. Barite is not typically toxic (Neff, 2002b) but other constituents of produced water can be toxic or radioactive, like radium-isotopes (Ra). Ba and Ra are chemical analogues and can co-precipitate

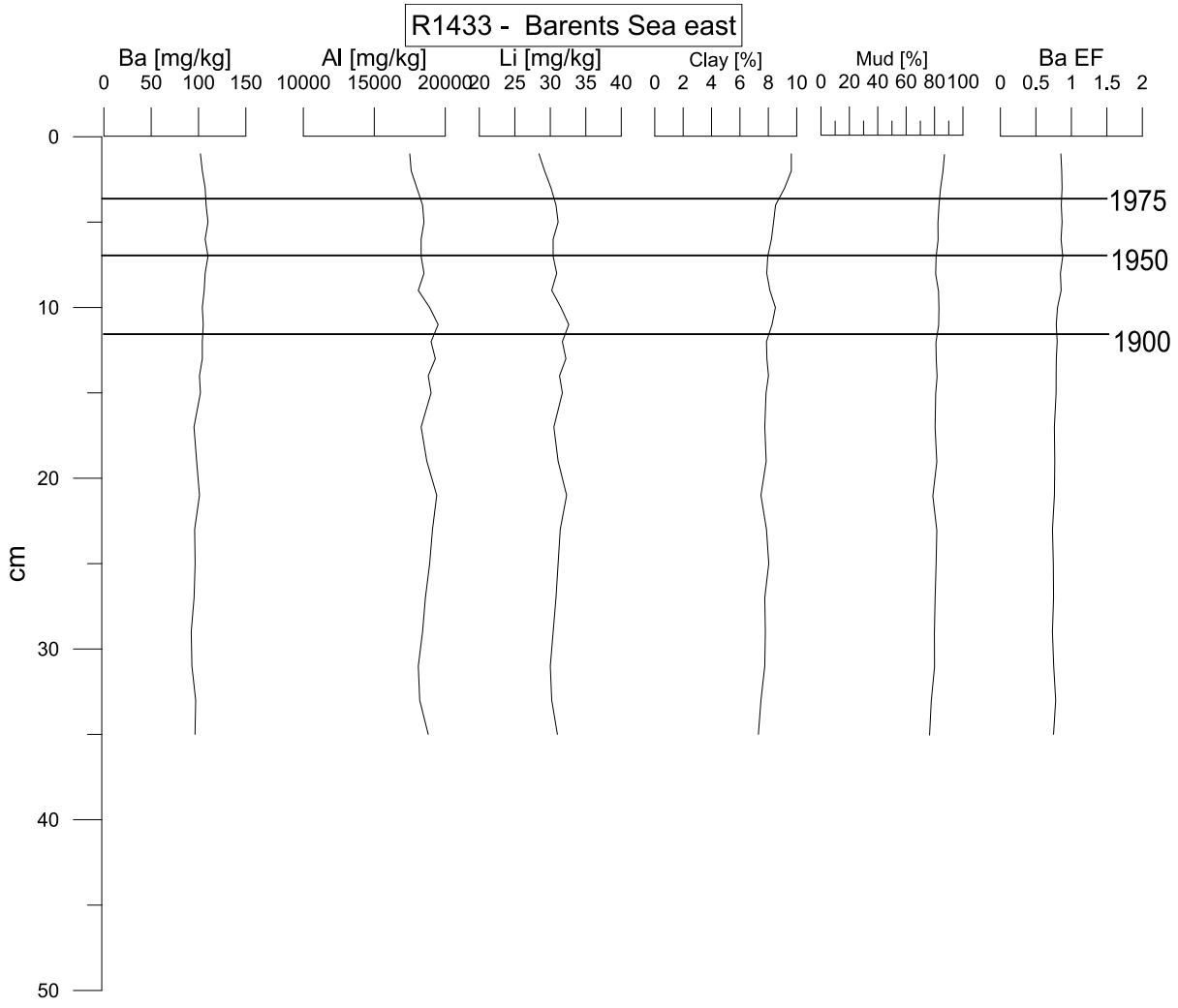

Fig. 14. ^{210}Pb-dated sediment core R1433 from Barents Sea east. Parameters include Ba, Al, Li, clay content, mud content and barium enrichment factor (EF). No significant changes are seen in Ba-concentrations or barium enrichment factor (Ba EF) down through the core. Ages are marked as lines at three depths.

Table 2
Parameter estimates, standard error (SE) and results for the terms of the linear regression model (adj $R^2 = 0.81$, $F(11, 2668) = 1023$, $p << 0.001$) for variation in amount of Ba in all studied samples according to variation in the predictor variables: percent clay content (clay), percent silt content (silt), amount of aluminium (Al), amount of lithium (Li), depth of the core slice (sediment depth), water depth of sampling stations (water depth), and the grouping of area, with the intercept based on the Norwegian Sea and the other groups being continental slope (CS), western Barents Sea (BSW, central Barents Sea (BSC) and eastern Barents Sea (BSE). For the area groups, factor levels follow this order by increasing Ba level (Fig. 5), and Helmert contrasts are used to illustrate significant differences related to area proximity.

Parameter	Estimate	SE	t value	Pr(>|t|)
Intercept	−45.8	26.7	−1.7	<0.09
% Clay	0.75	0.66	1.1	<0.27
% Silt	0.56	0.09	6.1	<<0.0001
Water depth	0.04	0.002	15	<<0.0001
Al	0.009	0.0007	13	<<0.0001
Li	−3.47	0.39	−8.9	<<0.0001
Core depth	−0.40	0.08	−5.0	<<0.0001
Area: CS	41.7	1.82	23	<<0.0001
Area: BSW	−11.5	0.93	−12	<<0.0001
Area: BSC	11.2	0.98	11	<<0.0001
Area: BSE	−9.71	0.50	−20	<<0.0001
Latitude	0.87	0.39	2.2	<0.026

Table 3
Parameter estimates, standard error (SE) and results for the terms of the linear regression model (adj $R^2 = 0.67$, $F(11, 2668) = 488$, $p << 0.001$) for variation in Ba enrichment factor in all studied samples according to variation in predictor variables: percent clay content (clay), percent silt content (silt), amount of aluminium (Al), amount of lithium (Li), depth of the core slice (core depth), water depth of sampling stations (water depth), and the grouping of area, with the intercept based on the Norwegian Sea and the other groups being continental slope (CS), western Barents Sea (BSW, central Barents Sea (BSC) and eastern Barents Sea (BSE). For the area groups, factor levels follow this order by increasing Ba level (Fig. 5), and Helmert contrasts are used to illustrate significant differences related to area proximity.

Parameter	Estimate	SE	t value	Pr(>|t|)
Intercept	1.30	0.24	5.6	<<0.0001
% Clay	−0.01	0.006	−1.9	<0.07
% Silt	0.004	0.0008	4.5	<<0.0001
Water depth	0.0003	0.00002	13	<<0.0001
Al	−0.000004	0.000006	−0.6	<0.54
Li	−0.017	0.003	−4.8	<<0.0001
Core depth	−0.005	0.0007	−7.4	<<0.0001
Area: CS	0.45	0.016	28	<<0.0001
Area: BSW	−0.07	0.008	−8.6	<<0.0001
Area: BSC	0.11	0.009	13	<<0.0001
Area: BSE	−0.07	0.004	−16	<<0.0001
Latitude	0.001	0.003	0.3	<0.77

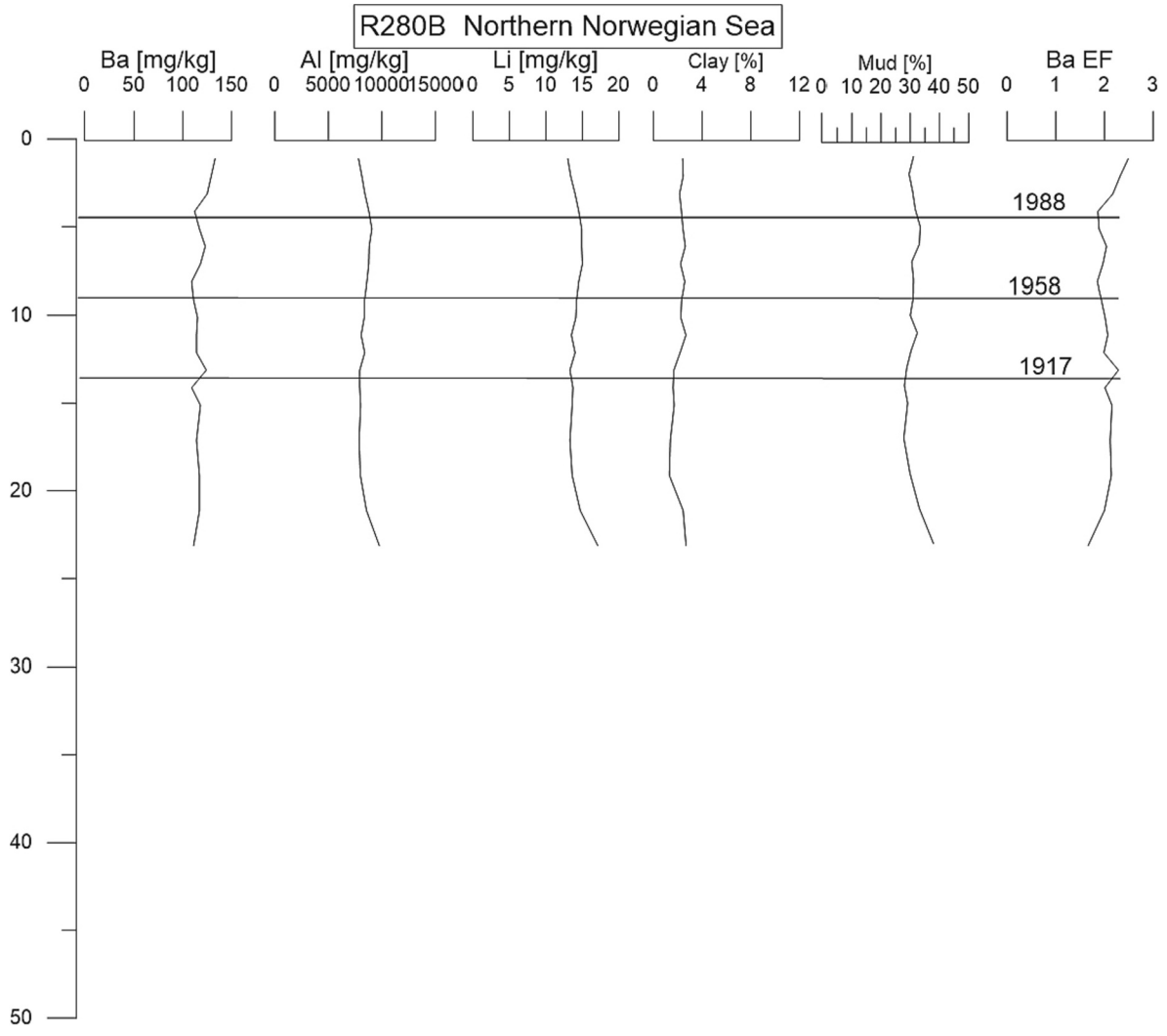

Fig. 15. ^{210}Pb-dated sediment core R280B from the Norwegian Sea. Parameters include Ba, Al, Li, clay content, mud content and barium enrichment factor (EF). There is a minor increase in Ba-concentrations and barium enrichment factor (Ba EF) from 1988. ^{210}Pb ages are marked as lines at three depths.

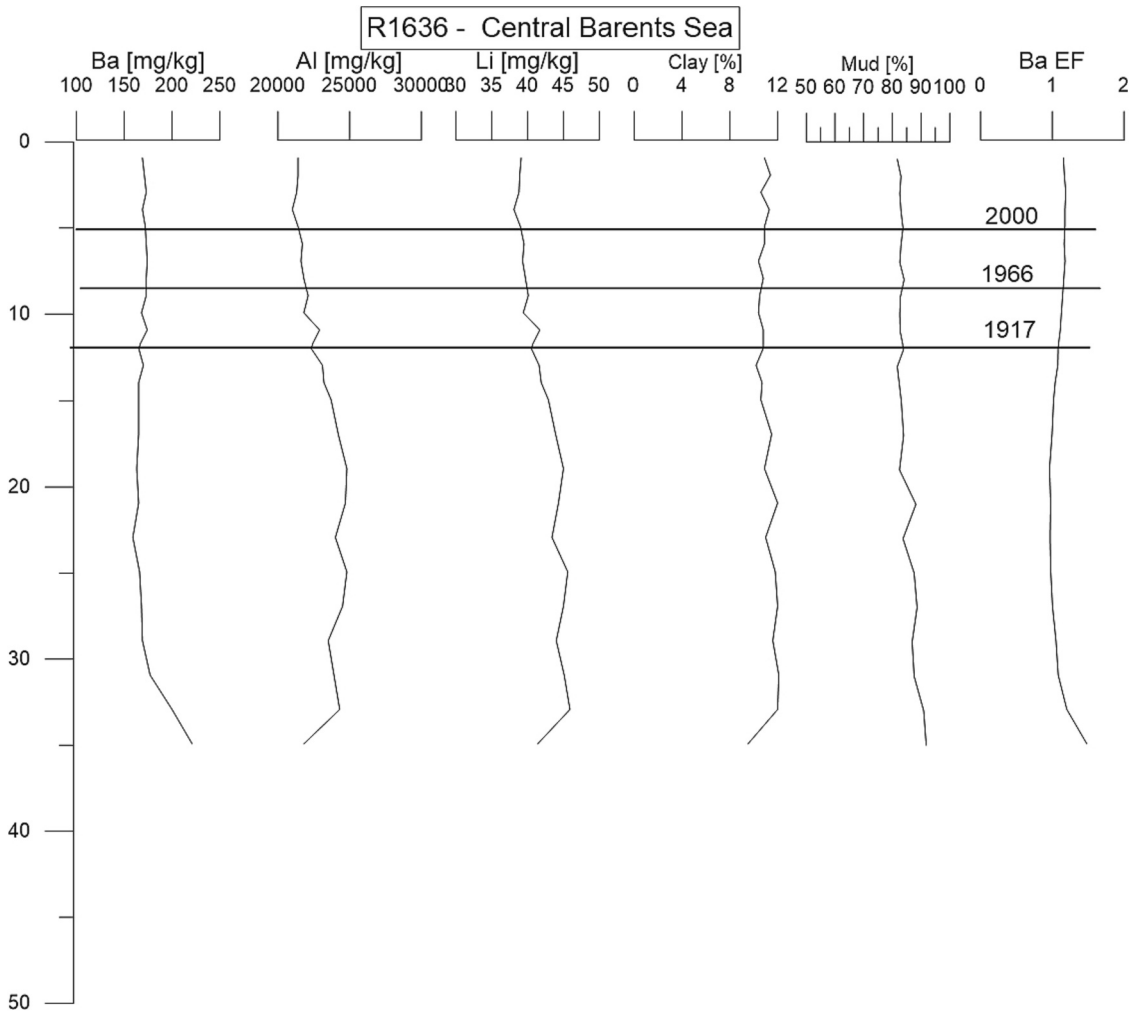

Fig. 16. ^{210}Pb-dated sediment core R1636 from central Barents Sea. Parameters include Ba, Al, Li, clay content, mud content and barium enrichment factor (EF). ^{210}Pb ages are marked as lines at three depths.

and form radiobarite (Neff et al., 1995). At the UK site, it was micron-sized radiobarite that was formed from produced water discharge (Ahmad et al., 2021). Sediments enriched in barite could thus be expected to also be enriched in Ra. Due to large discharge volumes of produced water, even low activity concentrations of Ra can sum up to large activity discharges. Ra discharges have been assessed, but due to few published data and many natural sources, evidence of impact from hydrocarbon drilling and production is lacking (Dowdall and Lepland, 2012; NRPA, 2004; Skjerdal et al., 2020). Since data on Ba in marine sediments are much more abundant, it is feasible to instead assess Ba variations in marine sediments. A modelling study indicates that the distribution of particle-associated Ra (radiobarite) behaves as barite, and indicate long distance dispersal (Reed and Hetland, 2002; Reed and Rye, 2011). However, field studies confirming this are lacking. In principle, it is difficult to distinguish between Ba originating from produced water versus drilling mud, but the latter should be less important due to its high density and should be more important in near-field plumes close to installations. Since MAREANO samples are not sampled near such installations or within near-field plumes, the overall picture from our results at more distant sites most probably reflects mainly Ba increases from discharges of produced water and possibly from the finer fractions of released drilling mud.

Since any impact may affect biological productivity and spawning in important fishery areas like Lofoten in the Norwegian Sea and the Barents Sea, the results of the study at hand suggests further investigations of the recent marine sediments to identify areas with enhancement of toxicants, like Ra. Modelling dispersal and sedimentation of particulate barite from hydrocarbon drilling and production using the DREAM model predicts an impact in the area of Lofoten (Reed and Hetland, 2002; Reed and Rye, 2011). Interestingly, this study also indicates increased Ba in the upper 6 cm in this area (Fig. 9). In addition, we find enhancements of Ba in other locations in the Norwegian Sea, at the continental slope and in the western Barents Sea. To make sure all natural sources are accounted for and to verify our results, further work should include toxicants like Ra, more elements specific to hydrocarbon drilling and especially production, and a larger geographical area.

6. Conclusions

In this study, we show that recent marine sediments in some areas in the Norwegian and Barents Seas have a higher-than-expected content of barium (Ba). Our findings coincides in age with the onset of the oil and gas industry. The results are found both for Ba concentrations alone and when accounting for Ba in detrital matter. We also find clear signals of input of Ba from natural sources like a mud volcano. Some samples with intermediate Ba enrichment may actually be impacted, since the values of other assessed variables would suggest much lower Ba enrichment. The areas we identify coincide with areas previously modelled as likely to receive such impact, giving support to our results. However, we also find additional areas that may be impacted. Many of the identified areas are close to, or at, important fish spawning or fishing grounds.

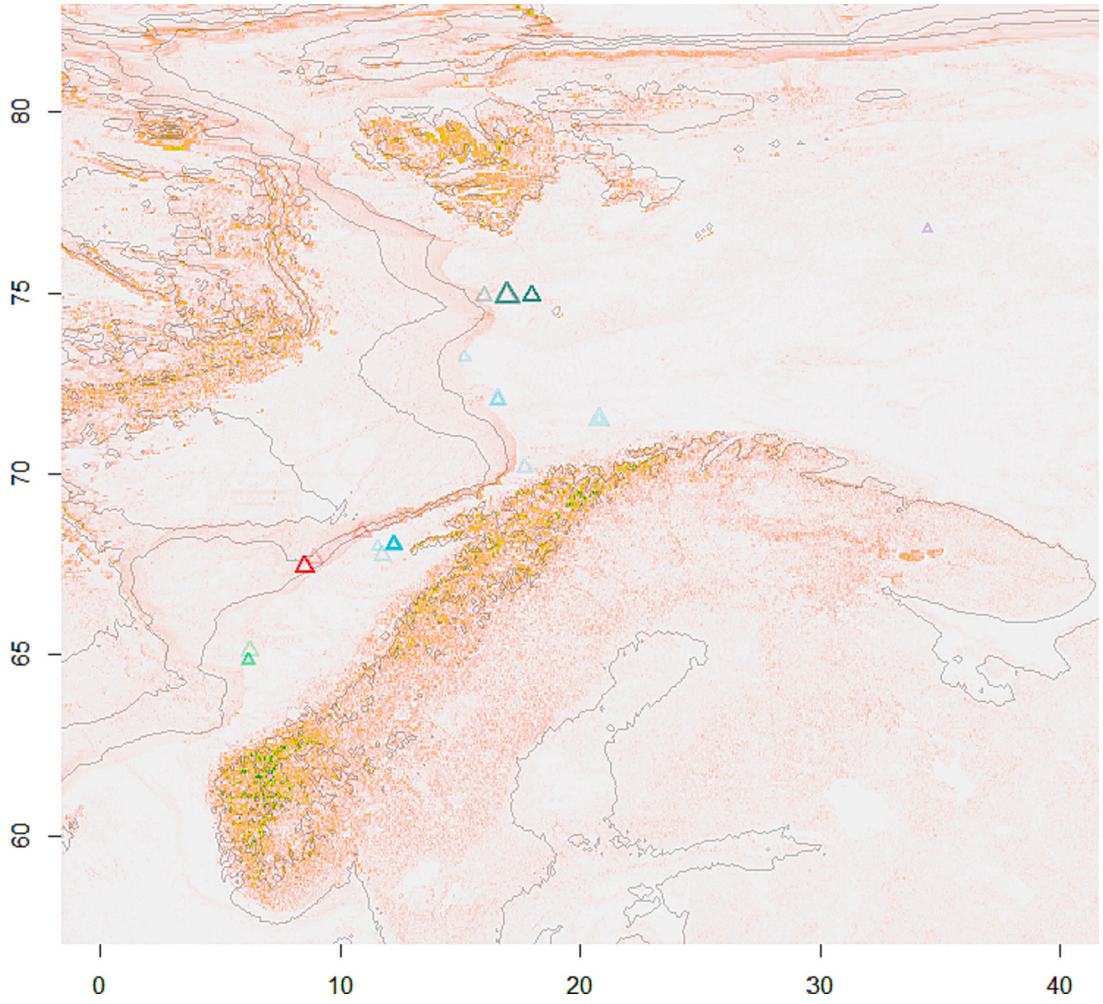

Fig. 17. Locations of studied sediment samples (triangles) with Ba enrichment factor (EF) more than one standard deviation larger than predicted from statistical model, with cex equal to EF/2. Samples from different areas are indicated by colours, with the Norwegian Sea south in green, the continental slope in red, the Barents Sea south-west and Norwegian Sea north in light blue, the Barents Sea north and central in green, and the Barents Sea south-east in purple. Different numbers of samples at one point give different colour intensities. Decimal degrees on axis for longitudes (X) and latitudes (Y). (For interpretation of the references to colour in this figure legend, the reader is referred to the web version of this article.)

CRediT authorship contribution statement

Hallvard Haanes: Conceptualization, Methodology, Validation, Investigation, Resources, Writing – original draft, Software, Formal analysis, Data curation, Visualization, Project administration. **Henning K.B. Jensen:** Conceptualization, Methodology, Validation, Investigation, Resources, Writing – original draft, Data curation, Visualization. **Aivo Lepland:** Conceptualization, Methodology, Validation, Investigation, Resources, Writing – original draft. **Hilde Elise Heldal:** Conceptualization, Methodology, Validation, Investigation, Resources, Writing – original draft, Visualization, Project administration, Funding acquisition.

Declaration of competing interest

The authors declare that they have no known competing financial interests or personal relationships that could have appeared to influence the work reported in this paper.

Data availability

Data will be made available on request.

Acknowledgements

The NORM project has received financial support from the Fram Centre Flagship Hazardous Substances. We thank the GEBCO Compilation Group (2022) for being able to download and use bathymetric map data. We thank Tanya H Hevrøy for spelling and grammar proofreading.

References

Ahmad, F., Morris, K., Law, G.T.W., Taylor, K.G., Shaw, S., 2021. Fate of radium on the discharge of oil and gas produced water to the marine environment. Chemosphere 273, 129550.

Bivand, R., Keitt, T., Rowlingson, B., 2019. rgdal: bindings forthe 'Geospatial' data abstractation library. R package version 1.4-4. https://CRAN.R-project.org/package=rgdal.

Bivand, R., Rundel, C., 2012. rgeos: Interface to Geometry Engine-Open Source (GEOS). R Package Version 0.2-2.

Brown, J., Colling, A., Park, D., Phillips, J., Rothery, D., Wrigth, J., 1995. The Ocean Basins: Their Structure and Evolution. Pergamon Press in association with The Open University, Milton Keynes, UK.

Brown, J., Colling, A., Park, D., Phillips, J., Rothery, D., Wrigth, J., 1995. Ocean Chemistry and Deep-sea Sediments. Pergamon Press in association with The Open University, Milton Keynes, UK.

Bøe, R., Dolan, M., Thorsnes, T., Lepland, A., Olsen, H., Totland, O., Elvenes, S., 2010. Standard for geological seabed mapping offshore. NGU report no. 2010.033. In: Geological Survey of Norway (NGU), p. 15.

Celis-Hernandez, O., Rosales-Hoz, L., Cundy, A.B., Carranza-Edwards, A., Croudace, I.W., Hernandez-Hernandez, H., 2018. Historical trace element accumulation in marine

sediments from the Tamaulipas shelf, Gulf of Mexico: an assessment of natural vs anthropogenic inputs. Sci. Total Environ. 622–623, 325–336.
Damm, E., Budéus, G., 2003. Fate of vent-derived methane in seawater above the Håkon Mosby mud volcano (Norwegian Sea). Mar. Chem. 82, 1–11.
de Haas, H., Boer, W., van Weering, T.C.E., 1997. Recent sedimentation and organic carbon burial in a shelf sea: the North Sea. Mar. Geol. 144, 131–146.
Dowdall, M., Lepland, A., 2012. Elevated levels of radium-226 and radium-228 in marine sediments of the norwegian trench ("Norskrenna") and Skagerrak. Mar. Pollut. Bull. 64, 2069–2076.
Egorov, A.V., Crane, K., Vogt, P.R., Rozhkov, A.N., Shirshov, P.P., 1999. Gas hydrates that outcrop on the sea floor: stability models. Geo-Mar. Lett. 19, 68–75.
Fischer, K., Puchelt, H., 1972. Chapter 56 - Barium, Handbook of geochemistry. Springer Verlag, Berlin, Heidelberg.
Frost, T., Myrhaug, J., Ditlevsen, M., Rye, H., 2014. Environmental Monitoring and Modeling of Drilling Discharges at a Location With Vulnerable Seabed Fauna: Comparison Between Field Measurements and Model Simulations.
Griffith, E.M., Paytan, A., 2012. Barite in the ocean – occurrence, geochemistry and palaeoceanographic applications. Sedimentology 59, 1817–1835.
Heldal, H.E., Varskog, P., Føyn, L., 2002. Distribution of selected anthropogenic radionuclides (137Cs, 238Pu, 239,240Pu and 241Am) in marine sediments with emphasis on the Spitsbergen-Bear Island area. Sci. Total Environ. 293, 233–245.
Hijmans, R., van Etten, J., 2012. Geographic Analysis and Modeling With Raster Data. R Package Version 2, 1-25.
Hjelstuen, B.O., Eldholm, O., Faleide, J.I., Vogt, P.R., 1999. Regional setting of Håkon Mosby mud volcano, SW Barents Sea margin. Geo-Mar. Lett. 19, 22–28.
Hjelstuen, B.O., Eldholm, O., Skogseid, J., 1997. Vøring plateau diapir fields and their structural and depositional settings. Mar. Geol. 144, 33–57.
Hovland, M., Nygaard, E., Thorbjørnsen, S., 1998. Piercement shale diapirism in the deep-water vema dome area, Vøring basin, offshore Norway. Mar. Pet. Geol. 15, 191–201.
Jensen, H.K.B., Bellec, V., 2021. In: Miljøkjemiske data og dateringsresultater fra Norskehavet., NGU-rapport 2021.028, MAREANO, p. 70.
Knies, J., Jensen, H.K.B., Finne, T.E., Lepland, A.,, 2006. Sediment Composition and Heavy Metal Distribution in Barents Sea Surface Samples: Results From Institute of Marine Research 2003 and 2004 Cruises., NGU-report 2006.067.
Lepland, A., Mortensen, P.B., 2008. Barite and barium in sediments and coral skeletons around the hydrocarbon exploration drilling site in the Træna deep, Norwegian Sea. Environ. Geol. 56, 119–129.
Lepland, A., Sæther, O., Thorsnes, T., 2000. Accumulation of barium in recent Skagerrak sediments: sources and distribution controls. Mar. Geol. 163, 13–26.
Loring, D.H., Rantala, R.T.T., 1992. Manual for the geochemical analyses of marine sediments and suspended particulate matter. Earth Sci. Rev. 32, 235–283.
Maiti, K., Carroll, J., Benitez-Nelson, C.R., 2010. Sedimentation and particle dynamics in the seasonal ice zone of the Barents Sea. J. Mar. Syst. 79, 185–198.
Milkov, A.V., 2000. Worldwide distribution of submarine mud volcanoes and associated gas hydrates. Mar. Geol. 167, 29–42.
Neff, J.M., 2002. In: Chapter 1 - Produced Water, Bioaccumulation in Marine Organisms. Elsevier, Oxford, pp. 1–35.
Neff, J.M., 2002. In: Chapter 4 - Barium in the Ocean, Bioaccumulation in Marine Organisms. Elsevier, Oxford, pp. 79–87.
Neff, J.M., 2008. Estimation of bioavailability of metals from drilling mud barite. Integr. Environ. Assess. Manag. 4, 184–193.
Neff, J.M., Sauer, T.C., Little, A.D.J., 1995. Barium in Produced Water: Fate and Effects in the Marine Environment, API Publication Number 4633. US Health and Environemtal Sciences Department, American Petroleum Institute, Cambridge, MA.
NRPA, 2004. Natural Radioactivity in Produced Water From the Norwegian Oil and Gas Industry in 2003., StrålevernRapport 2005:2. Statens strålevern, Østerås.
Pebesma, E., 2018. Simple features for R: standardized support for spatial vector data. R J. 10, 439–446.
Pebesma, E.J., Bivand, R.S., 2005. Classes and methods for spatial data in R. R News 5, 9–13.
R Core Team, 2016. Vienna, Austria. URL. In: Computing, R.F.f.S (Ed.), R: A Language and Environment for Statistical Computing. https://www.R-project.org/.
Reed, M., Hetland, B., 2002. In: DREAM: a Dose-Related Exposure Assessment Model Technical Description of Physical-Chemical Fates Components, SPE International Conference on Health, Safety and Environment in Oil and Gas Exploration and Production. Society of Petroleum Engineers, Kuala Lumpur, Malaysia, p. 23.
Reed, M., Rye, H., 2011. The DREAM model and the environmental impact factor: decision support for environmental risk management. In: Lee, K., Neff, J. (Eds.), Produced Water: Environmental Risks and Advances in Mitigation Technologies. Springer New York, New York, NY, pp. 189–203.
Reimann, C., Undersøkelse, N.G., Tutkimuskeskus, G., 1998. Environmental Geochemical Atlas of the Central Barents Region. Geological Survey of Norway.
Reitz, A., Pfeifer, K., de Lange, G.J., Klump, J., 2004. Biogenic barium and the detrital Ba/Al ratio: a comparison of their direct and indirect determination. Mar. Geol. 204, 289–300.
Rye, H., Brönner, U., Ditlevsen, M., Frost, T., Furuholt, E., Kjeilen-Eilertsen, G., Nepstad, R., Page, P., Paulsen, J., Ramos, R., Rønningen, P., Sorstrom, S.E., 2014. In: Use of the DREAM Model for Control and Prediction of Concentrations and Environmental Risks Associated with Regular Discharges to Sea: Experiences and Challenges. Proceedings - SPE Annual Technical Conference and Exhibition, 4, pp. 2510–2521.
Rye, H., Reed, M., Durgut, I., Arzlanoglu, Y., Brørs, B., Ditlevsen, M., Hetland, B., Smit, M., Frost, T., 2011. Environmental risk assessment of discharges from onshore facilities to coastal environments. In: International Conference on Health, Safety and Environment in Oil and Gas Exploration and Production, pp. 138–146.
Rye, H., Reed, M., Durgut, I., Ditlevsen, M.K., 2006. ERMS Report No. 18: Documentation Report for the Revised DREAM Model. SINTEF Materials and Chemistry, Trondheim, Norway.
Singsaas, I., Rye, H., Frost, T., Smit, M., Garpestad, E., Skare, I., Bakke, K., Veiga, L., Buffagni, M., Follum, O.-A., Johnsen, S., Moltu, U.-E., Reed, M., 2008. Development of a risk-based environmental management tool for drilling discharges. Summary of a four-year project. Integr. Environ. Assess. Manag. 4, 171–176.
Skjerdal, H., Heldal, H.E., Rand, A., Gwynn, J., Jensen, L.K., Volynkin, A., Haanes, H., Møller, B., Liebig, P.L., Gäfvert, T., 2020. Radioactivity in the Marine Environment 2015, 2016 and 2017. Results from the Norwegian Marine Monitoring Programme (RAME). , DSA StrålevernRapport 2020:04. Norwegian Radiation and Nuclear Safety Authority, Østerås.
Smith, J.N., Ellis, K.M., Naes, K., Dahle, S., Matishov, D., 1995. Sedimentation and mixing rates of radionuclides in Barents Sea sediments off Novaya Zemlya. Deep-Sea Res. II Top. Stud. Oceanogr. 42, 1471–1493.
Thorsnes, T., Bellec, V., Baeten, N., Plassen, L., Bjarnadottìr, L.R., Ottesen, D., Dolan, M., Elvenes, S., Rise, L., Longva, O., Bøe, R., Lepland, A., 2016. Mid-Norwegian continental shelf and slope. In: Uhl-Mortensen, L., Hodnesdal, H., Thorsnes, T. (Eds.), The Norwegian Sea Floor,. MAREANO Program, p. 192.
Tribovillard, N., Algeo, T.J., Lyons, T., Riboulleau, A., 2006. Trace metals as paleoredox and paleoproductivity proxies: an update. Chem. Geol. 232, 12–32.
Vogt, P., Cherkashov, G., Ginsburg, G., Ivanov, G., Milkov, A., Sundvor, A., Pimenov, N., Egorov, A., 1997. Haakon Mosby mud volcano provides unusual example of venting. EOS Trans. Am. Geophys. Union 78, 549-549.
Vorren, T.O., Richardsen, G., Knutsen, S.-M., Henriksen, E., 1991. Cenozoic erosion and sedimentation in the western Barents Sea. Mar. Pet. Geol. 8, 317–340.
Xu, R., 2000. Characterization. Light Scattering Methods. Kluwer Academic Press, Massachusetts.
Yang, J., Wang, W., Zhao, M., Chen, B., Dada, O.A., Chu, Z., 2015. Spatial distribution and historical trends of heavy metals in the sediments of petroleum producing regions of the beibu gulf, China. Mar. Pollut. Bull. 91, 87–95.
Zaborska, A., Carroll, J., Papucci, C., Torricelli, L., Carroll, M.L., Walkusz-Miotk, J., Pempkowiak, J., 2008. Recent sediment accumulation rates for the Western margin of the Barents Sea. Deep-Sea Res. II Top. Stud. Oceanogr. 55, 2352–2360.